

This is a non-peer reviewed pre-print submitted to EarthArXiv. Subsequent versions of this manuscript may have slightly different content. The manuscript has been submitted to The Geological Society Special Publications - Oceanic Gateways: Modern and Ancient Analogues and their Conceptual and Economic Implications for peer-review.

5

Seismic stratigraphy of the Guinea Plateau before, during and after the opening of the Equatorial Atlantic Gateway

10 **Benedict Aduomahor**¹ (boa3@hw.ac.uk) @truman_119, **Debora Duarte**¹ (d.pascoal_duarte@hw.ac.uk)
@niobsidian, **Thomas Wagner**² (t.wagner@hw.ac.uk), **Tom Dunkley Jones**³ (t.dunkleyjones@bham.ac.uk)
@TomDunkleyJones, **Uisdean Nicholson**^{1,a} (u.nicholson@hw.ac.uk) @EileanClach

¹*School of Energy, Geoscience, Infrastructure and Society (EGIS), Heriot-Watt University, Edinburgh*

15 ²*Lyell Centre Global Research Institute, Heriot-Watt University, Edinburgh*

³*School of Geography, Earth and Environmental Science, University of Birmingham*

^aCorresponding author: u.nicholson@hw.ac.uk

20

25

30

35

40

Abstract:

The Guinea Plateau contains a ~200-million-year stratigraphic record, encompassing the mid-Cretaceous opening of the Equatorial Atlantic Gateway (EAG). Here we present new 2D seismic data to constrain the structural and stratigraphic evolution of the plateau. Seismic stratigraphic analysis reveals five megasequences of ~25-65 My duration: M1, a Jurassic syn-rift sequence with prominent seaward-dipping reflections; M2, a late Jurassic- Early Cretaceous post-rift carbonate platform; M3, a late Early Cretaceous syn-transform clastic-dominated sequence; M4, an Albian-Maastrichtian post-transform sequence; and M5, a Maastrichtian-Recent passive margin sequence with low sedimentation rates. These megasequences also contain prominent transgressive-regressive cycles of 5-10 My duration, interpreted to be the result of dynamic topography.

The boundary between M3 and M4 is a major erosional unconformity documenting final continental breakup during the opening of the EAG. Above this, a pronounced Albian to Cenomanian/Turonian marine transgression resulted in marine inundation of the plateau. Structural deformation continued into the early Cenomanian along the Guinea Marginal Ridge, a potential structural barrier that restricted marine connection across the EAG. Bulk geochemical data from the shallow Guinea Plateau indicate that enhanced carbon burial in this setting was primarily driven by the deposition of reworked, oxidised organic matter during OAE, independent of gateway opening.

Keywords: Seismic stratigraphy, sediment routing, black shales, ocean gateway, Equatorial Atlantic Gateway (EAG),

1. Introduction

The Guinea Plateau is a major promontory of continental crust located in the equatorial West African passive margin, offshore Guinea and Guinea-Bissau (Fig. 1). The conjugate of this submarine marginal plateau on the South American plate is the Demerara Plateau off French Guiana and Suriname (Loncke et al., 2022, Graindorge et al., 2023). These conjugate plateaus formed during African - South American breakup, part of the longer-term breakup of western Gondwana (Mercier de Lépinay et al., 2016, Loncke et al., 2020).

The final separation of these continents in the mid-Cretaceous, and formation of the Equatorial Atlantic Gateway (EAG) (Moulin et al., 2010; Heine et al., 2013; Pérez-Díaz & Eagles, 2017), is the consequence of two major tectonic rifting phases, in the Jurassic and then in the Early Cretaceous (Masclé et al., 1988, Marinho et al., 1988a, Davison, 2005).

As well as influencing the stratigraphic evolution and sediment routing of the margin, the tectonic events that resulted in the opening of the EAG, exerted a strong influence on global palaeoceanography, palaeoclimatic and environmental changes (Biddle, 1985; Zimmerman et al., 1988; Wagner 2002; Louis-Schmid et al., 2007; Sijp et al., 2014; and Dummann et al., 2020). In particular, the geometry of these transform margins is more likely to produce structural barriers and temporal changes in gateway geometry conditions (Wagner & Pletsch, 1999; Voigt et al. 2013; Mourlot et al. 2018; and Laugié et al. 2021a). The opening of the EAG in the mid-Cretaceous coincided with extensive deposition and preservation of organic-rich shale with elevated Total Organic Carbon (TOC) across basins of the Central, North, and South Atlantic (Schlanger et al. 1987; Moullade et al. 1993; Meyers et al. 2006; Jones et al. 2007; Topper et al. 2011; Berrocoso et al. 2010a; Casson et al. 2021; Laugié et al. 2021). The narrow and restricted basins of the Central Atlantic limited deep marine connections, water mass circulation and ventilation (Wagner & Pletsch, 1999, Voigt et al. 2013; Mourlot et al. 2018; Laugié et al. 2021) which combined with high, orbitally-modulated continental runoff of nutrient-rich waters

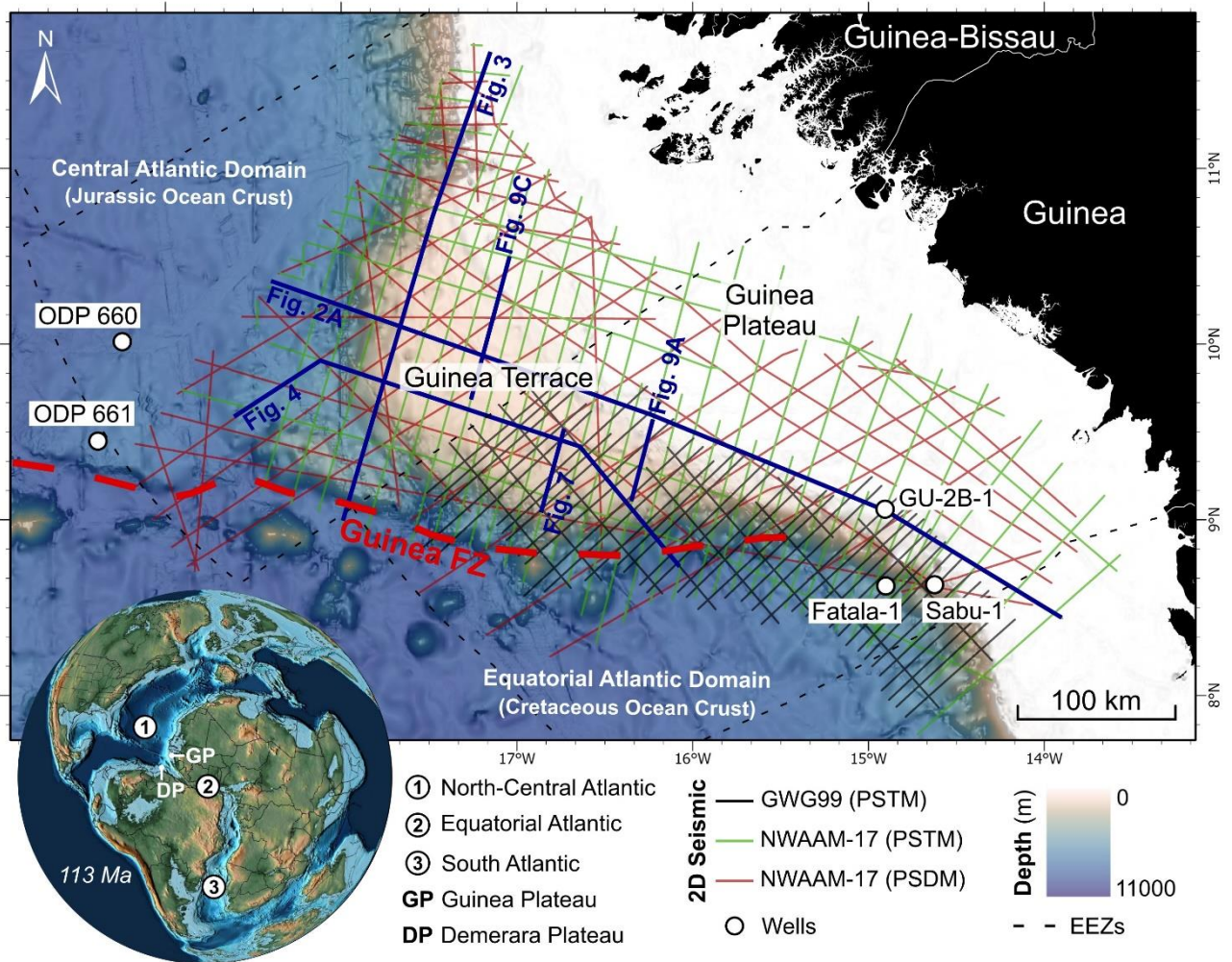
preconditioned these regions to enhanced organic matter production and preservation (Hoffmann et al. 2003, Wagner et al. 2004, Wagner 2006, Lowery C. et al., 2021). Distinguishing the impacts of changing tectonic boundary conditions versus long-term climate evolution on marine biogeochemistry requires reliable reconstructions of the tectonic evolution of the Central Atlantic conjugate margins through rifting and breakup. Here we use new seismic stratigraphy to contribute to this effort for the Guinea Plateau.

Despite the Guinea Plateau's important position at the transition between the Jurassic Central and Cretaceous Equatorial Atlantic continental margins, the stratigraphic evolution of the plateau is not well constrained. Previous work has focused on the structural evolution of the Southern Guinea margin, highlighting the presence of upper-crustal asymmetry and depth-dependent stretching in the conjugate Guinea and Demerara margin during Cretaceous rifting (Olyphant et al, 2017). The stratigraphic framework used in Olyphant et al. (2017), did not, however, capture the complex transform tectonics and the resultant sedimentation patterns observed across the Guinea margin. In this study, we investigate new regional 2D seismic data across the entire Guinea margin to understand the structural and stratigraphic characteristics of the plateau before, during and after the opening of the EAG. We define a regional high-resolution stratigraphic framework of the Jurassic to Recent sediments, including calculation of sediment accumulation rates through time, to reconstruct the interplay between tectonic, geodynamic, eustatic, and sedimentary processes that controlled deposition on the Guinea Plateau at different timescales. We then look at the local structural and stratigraphic characteristics of the mid-Cretaceous sequence on the plateau in more detail, to understand the role that the tectonic boundary conditions of the emerging gateway had on ocean circulation and ventilation.

1.1 Regional Geological Setting

The Guinea Plateau is a major submarine geomorphological feature that lies along the West African coastline, offshore Guinea and Guinea Bissau, between a latitude of 7 – 11°N. It extends to over 400 km off the coast, with water depths ranging from 15 – 1400 m. The plateau includes a thick sedimentary basin that is a part of the contiguous Mauritania-Senegal-Gambia-Guinea Bissau-Guinea Conakry (MSGBC) Basin located along the NW African Atlantic margin (Davison, 2005). The sub-basins are aligned in a north-south orientation along the continental margin, in Mauritania, Senegal, The Gambia, Guinea Bissau and Guinea, and are bounded by the Cap Blanc Fracture zone to the north and the Guinea Fracture Zone to the south. The Guinea Plateau is bounded by two continent-ocean boundaries of distinctly different crustal ages. To the north of the GFZ, on the Central Atlantic domain, the oldest oceanic crust is of Jurassic age, whereas to the south of the GFZ, on the Equatorial Atlantic segment, the age of the oldest oceanic crust is Early Cretaceous (Basile, 2005). Both segments form an ocean-ocean boundary to the west of the Guinea Plateau where the oceanic crust of Jurassic and Upper Cretaceous age is juxtaposed along the GFZ (Fig. 1). The continental slope of the western part of the Plateau shows a general north-south trend, while the southern segment is marked by an approximate east-west trending steep slope. Both segments converge to the southwest of the plateau in an area with a steep and structurally

complex continental slope (Duarte et al., in review). This slope is controlled by the GFZ which continues eastwards into the northern margin of the Sierra Leone basin parallel to a chain of aligned seamounts.



5 **Figure 1.** Bathymetry map of the Guinea margin showing location of the study area and the dataset used for this study. 2D seismic line locations and three exploration wells (*Fatala-1*, *Sabu-1* and *GU2B-1* wells) are shown, with line locations for seismic profiles in later figures highlighted.

The Guinea margin formed during multiple distinct tectonic phases that led to the break-up of western Gondwana (Marinho et al., 1988; Rossi et al., 2001.) The first was the Jurassic opening of the Central Atlantic Ocean and the formation of the Central Atlantic passive margin, with rifting events initiated between the Early to Late Triassic (Davison, 2005). The second event was the northward-propagating Cretaceous opening of the Southern Atlantic (Heine et al., 2013). The final separation between Africa and South America, to form the Equatorial Atlantic, in the Early Cretaceous was a consequence of lithospheric extension that resulted in the formation of a series of large intracontinental rift systems (Moulin et al., 2010; Heine et al., 2013; Heine & Brune, 2014). The GFZ formed by intracontinental transform faulting during the Cretaceous rift phase (Basile

& Mascle, 1990; Marinho et al., 1988), initiating in the early Albian between the Demerara and Guinea Plateaus (Heine et al., 2013; Moulin et al., 2010). The Guinea Plateau continued to undergo structural deformation during this transform stage, as is typical for other transform margins (Benkhelil et al., 1998; Mercier de Lépinay et al., 2016), with the development of distinctive structural and topographic features. One of these features is a basement marginal ridge at the SE transform segment of the Guinea Plateau (Mascle et al., 1988). The formation mechanism and timing of this basement marginal ridge, and its influence on circulation in the emerging EAG, is not clearly understood and is a focus of this study.

Dataset and methods

2.1 Datasets

10 2.1.1. Seismic reflection data

This study uses geophysical and geological data acquired along the Guinea-Bissau and Guinea margins. The data include 2D regional seismic reflection data and petrophysical, bulk geochemical, and biostratigraphic data from two exploration wells (Fig. 1).

The 2D multichannel seismic reflection data were acquired and processed by TGS and Schlumberger from three surveys covering an area of approximately 198,000 km² of the Guinea margin with an average line spacing of 5.5 km. The NWAAM-17 surveys 1 and 2 in Guinea and Guinea Bissau were acquired by TGS in 2011 and 2017 respectively, in water depths of 15-4600 m. The GWG99 survey was acquired by Schlumberger in 1999, in water depths of 15–4000 m. The seismic data were processed using a Pre-Stack Time Migration (PSTM) sequence, with a subset of data in survey 2 and GWG 99 reprocessed to improve imaging and reduce multiples and noise. See Supplementary Material A1 for acquisition and processing parameters.

2.1.2. Well data: lithologies and biostratigraphy

Well data for this study come from two commercial boreholes in the east of the Guinea Plateau, the Sabu-1 and GU2B-1 wells (Fig. 1). Wireline log data and information on lithostratigraphy (cuttings description) and biostratigraphy were obtained from the commercial well reports. No physical samples were available for analysis.

The Sabu-1 well is an exploration well drilled in the offshore Guinea Basin in 2012, at a water depth of 707 m. The well was drilled to a total vertical depth (TVD) of 3599 m, where it encountered sediments of Albian age. The Sabu-1 well sequence consists of volcanic breccias, siltstones and thin beds of calcareous claystone in the Albian, with thin beds of calcareous claystone and volcanics close to the Albian unconformity. Overlying this is a sequence of interbedded carbonate and claystone, overlain by a thick sequence of Cenomanian to Turonian grey-brown shale. Siltstone, sands, and carbonates overlie the Turonian, up to the top of the Cretaceous. The Cenozoic sediments above these are Palaeocene limestones interbedded with layers of sands and claystone.

The GU2B-1 well is located on the southern edge of the Guinea plateau, drilled at water depth of ~100 m to a total depth of 3353 m TVD, where it encountered sediments of Barremian age. The GU2B-1 well consists

predominantly of sandstone, mudstones, carbonate and volcanic material (Fig. 2). The Barremian sequence comprises mudstone interbedded with sandstone. Above this sequence are deposits of the Aptian to Albian consisting of brown to grey claystone interbedded with sandstone, volcanics and volcanic breccias. The volcanic sequence extends up into the lowermost Cenomanian and is overlain by a thick package of Cenomanian and Turonian black shales, followed by Santonian to Maastrichtian interbedded sandstones, shales, and dolomitic sediments. An undisturbed Cenozoic sequence includes a thick Palaeocene-Eocene carbonate sequence truncated by an Oligocene unconformity, followed by Miocene to Recent sands and claystones, likely deposited in submarine canyons and channels.

10 2.2 Methods

2.2.1 *Seismic to well tie*

Well data in the depth domain was converted to the time domain for interpreting the seismic data, using checkshot data. Synthetic seismograms were generated to improve the seismic-to-well ties using both density and sonic logs in the GU2B-1 and Sabu-1 wells to generate acoustic impedance and reflection coefficient logs. The reflectivity coefficient was then convolved with a wavelet that was statistically extracted from the seismic sections intersected by the well. The synthetic seismogram was tied to the nearest seismic traces to the well trajectory to correlate well log data to the seismic volume. Well-to-seismic ties and seismic interpretation was carried out using Petrel E&P software (Schlumberger). See Supplementary Material A3 for seismic-to-well ties for the two wells.

20 2.2.2 *Seismic and Sequence Stratigraphic Analysis*

The seismic stratigraphic analysis follows the standard approach of Mitchum & Vail, (1977) and Emery and Myers (1996) including analysis of seismic facies and the characterization of reflection geometries (character of internal reflection, vertical and lateral variations, frequency, amplitude and reflection continuity). These analyses provide the basis for the seismic stratigraphic framework and depositional environment maps for each of the seismic units. See Supplementary Material A4 for the seismic facies scheme developed for this project.

Seismic stratigraphic analysis also includes the identification of transgressive and regressive packages from reflection terminations, such as clinoform packages and shelf-edge trajectory patterns. The shelf-edge trajectory trends were identified from the seismic data based on the interpretation of the successive position of the offlap breaks - the point of maximum curvature between the topset and foreset. A chronostratigraphic chart (Wheeler diagram) for the Guinea margin was built by mapping the lateral extent of seismic units, to characterise the depositional geometries and chronology of sedimentary events in the Guinea margin from the Jurassic to the Cenozoic.

2.2.3. Reconstruction of sediment accumulation rates

Seismic horizons were used to reconstruct a sediment budget for the Guinea Plateau and constrain changes in sediment accumulation through time. The workflow for this was adapted from Nicholson et al. (2016). The top and base of the mapped seismic units were gridded to generate regional surfaces across the Guinea Plateau. These were converted to depth using a time-depth relationship derived from the wells, and from pseudowells extracted from individual seismic profiles (see Supplementary Materials A5). For the pseudowells, processing velocities were extracted from the seismic velocities along a vertical trace. The seismic velocity was calibrated with the well checkshot velocity and a simple V_0+kZ function was extracted that was used to build a simple velocity model for time-to-depth domain conversion. The depth-converted data were used to generate isopach maps and gross volume for each seismic unit. A porosity correction (Sclater & Christie, 1980) was applied to convert these to solid rock volumes. These were then used to calculate sediment accumulation rates for each interval, by dividing the solid rock volume by the duration of the unit. Where absolute ages for seismic horizons were not available from the Guinea Plateau wells (Aptian and older), the age of seismic horizons was assumed by visual comparison of similar seismic facies from the Demarara Plateau (Casson et al., 2021). No sediment budget was calculated for carbonate rocks (M2) as the objective was to constrain terrestrial sediment flux to the basin through time.

The major uncertainties in estimating the sediment budget are the seismic horizon mapping across the Guinea margin ($u_1 = 10\%$), the uncertainty in assigning age horizons and major unconformities ($u_2 = 10\%$), velocity modelling ($u_3 = 10\%$), the domain conversion process ($u_4 = 7.5\%$), and porosity correction ($u_5 = 5\%$). These are used to calculate the overall uncertainty (u_T) using the Root Sum Square (RSS) method (Nicholson et al., 2016):

$$\text{RSS } (u_T) = \sqrt{(u_1^2 + u_2^2 + u_3^2 + u_4^2 + u_5^2)}$$

The overall uncertainty on sediment budget estimation is thus on the order of ~20%.

2.2.4 Bulk geochemical analysis

Bulk geochemical data for side wall cores and cuttings samples of GU2B-1 and Sabu-1 wells were extracted from the industry reports. These include Total Organic Carbon (TOC), thermal maturation (T_{max}) of the organic matter (for GU2B-1 only), vitrinite reflectance and other Rock Eval pyrolysis parameters - S1 (free hydrocarbon), S2 (hydrocarbon potential), S3 (CO_2 potential), HI (hydrogen index) and OI (oxygen index). These parameters were used to generate depth plots (TOC, T_{max}) and modified van Krevelen diagrams (HI and OI), that were used to determine the hydrocarbon generation potential, thermal maturity of organic matter (for GU2B-1 only), and to compare the quality of the source-rock and kerogen type. For the GU2B1 well, a total of 170 samples across ten chronostratigraphic units (from Oligocene to Barremian), covering a depth interval of 950-3352 m, were analyzed (Fig. 14). For the Sabu-1 well, 60 samples from the Cretaceous (Maastrichtian to Albian) were analyzed across the 2195-3595 m depth interval. Standard notations are applied: TOC, given in weight percent (%wt), S1 & S2 are given in milligram of hydrocarbon per gram of rock

(mgHC/gRock), S3 is in milligram of carbon dioxide per gram of rock (mgCO₂/gRock), Tmax is in °C, HI is expressed in mgHC/gTOC, and OI expressed in (mgCO₂/gTOC). For kerogen type assessment thermal maturity was considered while samples with TOC concentrations below 0.5% was excluded.

3. Results and interpretation

5 Sixteen seismic stratigraphic horizons were identified and mapped across the entire Guinea margin. The seismic horizons include four regional unconformities, the Jurassic (JU), early Albian (AU), Top Maastrichtian (K), and base Oligocene (OG) (Figs. 2-4). These unconformities are used to define five seismic megasequences (M1 – M5), or 1st order sequences (Catuneanu, 2019), of ~25-65 My duration. The other horizons define fifteen seismo-stratigraphic units (SU1-SU15) with an average duration of approximately 8-12 My, broadly
 10 corresponding to 2nd order sequences (Catuneanu, 2019).

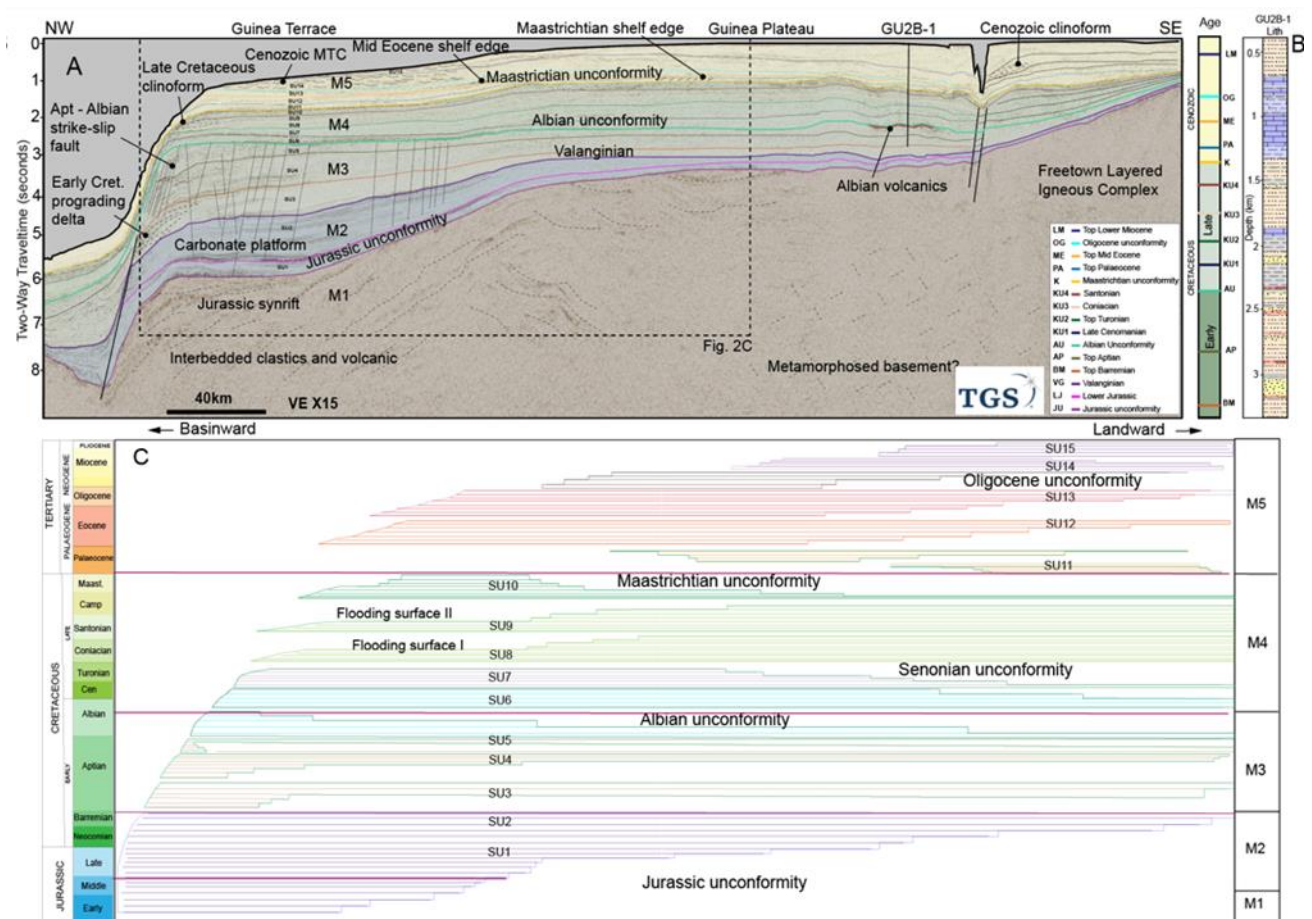
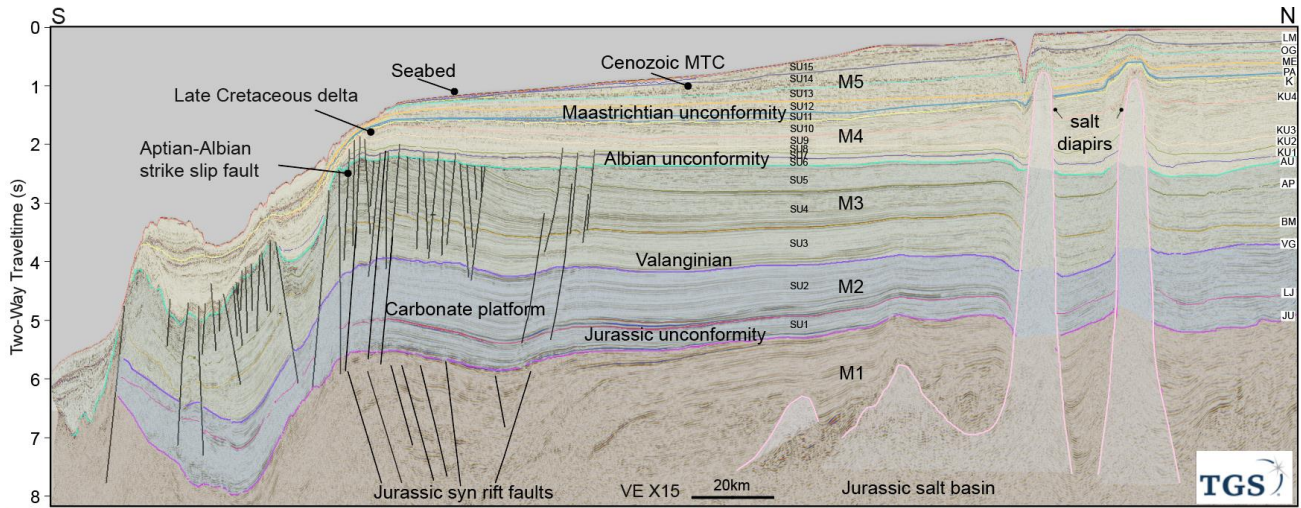


Figure 2. Interpreted 2D regional seismic line running from southeast to northwest across the Guinea Plateau, from shallow to deep water (location of line is given on the map in Fig. 1). (a) seismic line showing the sixteen interpreted horizons correlated with the GU2B-1 well, megasequences (M1 – M5) and 15 seismic units (SU1 – SU15). (b) lithological summary of the GU2B-1 well – see Supplementary Materials A2 for biostratigraphy and seismic markers. (c) Chronostratigraphic diagram showing the lateral extent of seismic
 15

reflections from line (b) showing areas of non-erosion and deposition (major sequence boundaries and flooding surfaces).



5 **Figure 3.** 2D seismic line running north to south - location of line shown on Fig. 1. The interpreted section shows megasequences (M1 – M5) and seismic units (SU1 – SU15). The Jurassic unconformity represents the Central Atlantic breakup unconformity, and the Albian unconformity the Equatorial Atlantic breakup unconformity respectively. The Albian breakup unconformity clearly separates the high-angle faulted sequence of M3 from the undeformed M4 sequence above. Note that the entire SU5 sequence is missing on the southern end of the Guinea Plateau, representing around 500 m of eroded sediment.

10

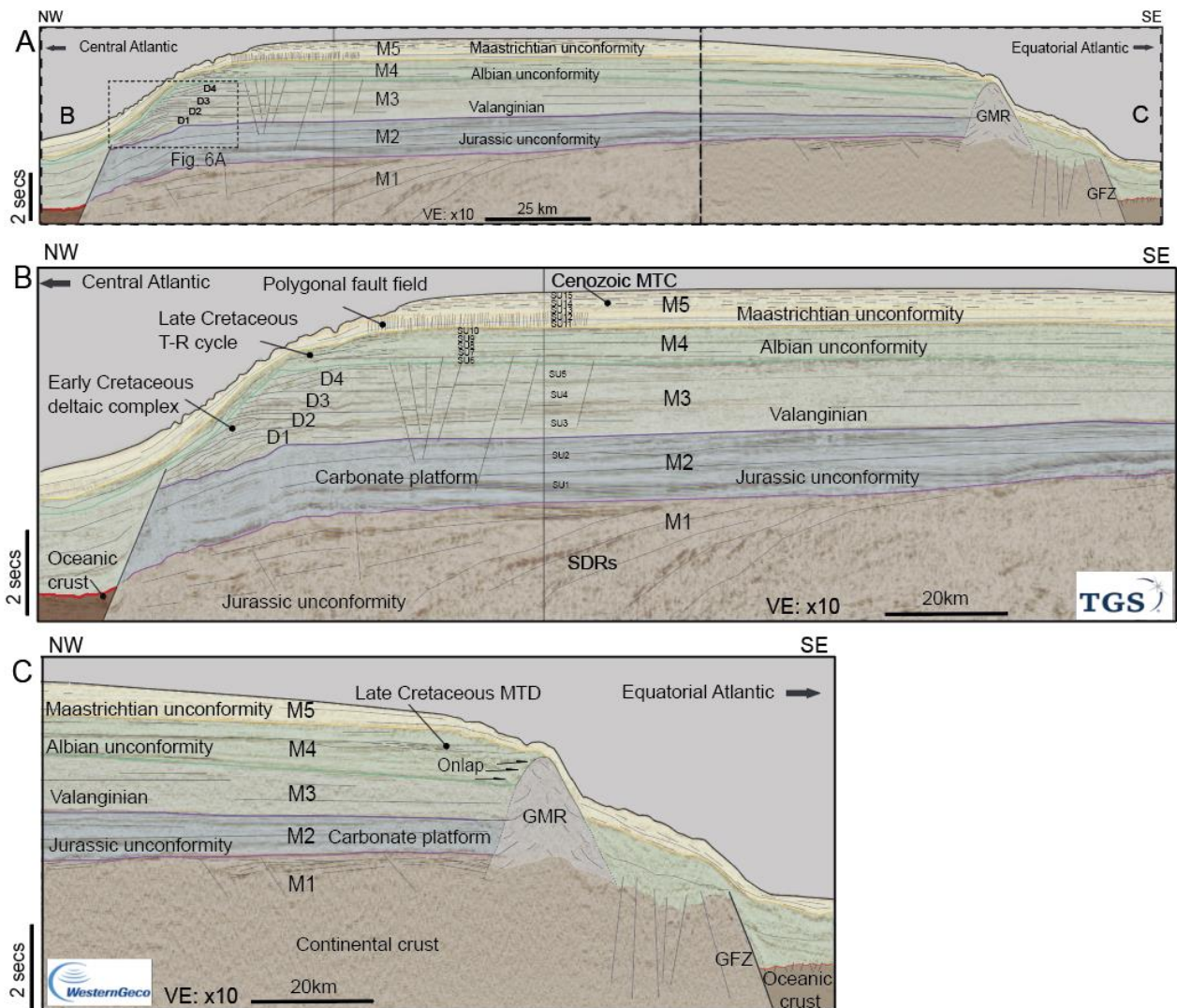


Figure 4. (A) 2D regional composite seismic line running from southeast to northwest across the Guinea Plateau, from the Equatorial domain to the Central Atlantic domain - location of line is given on the map in Fig. 1. (B) Inset from the regional line (A) showing the megasequences (M1 – M5) and 15 seismic units (SU1 – SU15). (C) Inset from the regional line (A), showing the Guinea Marginal Ridge (GMR) situated on the proximal side of the Guinea Fracture Zone (GFZ) formed from transpressional uplift.

3.1 Megasequence 1 (M1) - Jurassic syn-rift sequence

M1 is the deepest stratigraphic megasequence recognised in this study. The top of this sequence is marked by the JU reflector and its base is unmapped (Figs 2-4). The internal reflectors of this sequence show a range of different characteristics from discontinuous, low to medium-amplitude, sub-parallel reflections, to discontinuous, high-amplitude reflections. Oblique and dipping reflectors terminate at the JU reflector towards the south. Several sets of extensional faults are interpreted in this section. In the northern area of the plateau, a number of salt diapirs are identified, characterised by low reflectivity seismic facies with few internal reflections (Fig. 3). Towards the south of the Guinea Plateau, there are discrete packages of concave-downward, basinward (westward) dipping reflectors of medium to high amplitudes in this sequence (Figs. 2 and 4). These are

interpreted as seaward dipping reflectors (SDRs) characteristic of ocean-continent transition zones on volcanic margins.

3.2 Megasequence 2 (M2) - Central Atlantic post-rift sequence

5 The Central Atlantic post-rift sequence (M2) is interpreted from the top of the Jurassic syn-rift (JU reflector) to the top Valanginian (VG) reflector (Figs. 2-4). The LJ reflector forms the boundary between two separate seismic units, SU1 and SU2. Both seismic units have laterally continuous, high amplitude reflections that extend across the entire Guinea Terrace, being locally thicker to the west, and thin and pinch out onto the shallower Guinea Plateau to the east (Figs. 2 and 5).

10 The thick wedge-shaped depositional unit of M2 exhibits an increase in thickness towards the southwest, suggesting greater accommodation space in this area during deposition (Fig. 4, 5A). This corresponds to the area with SDRs, suggesting more pronounced post-rift thermal subsidence in this area during the early passive margin phase. No wells penetrate this interval on the Guinea margin. Wells drilled on the conjugate Demerara margin (Casson et al., 2021) and further to the north in the MSGBC Basin (Ko, 2018) penetrate carbonates in this equivalent sequence. The high-amplitude seismic facies on the Guinea Plateau are similar to those in the
15 Demerara Plateau, consistent with a carbonate platform. The decrease in amplitude to the east likely corresponds to an eastward increase in clastic, continentally derived sediment component closer to the continental margin.

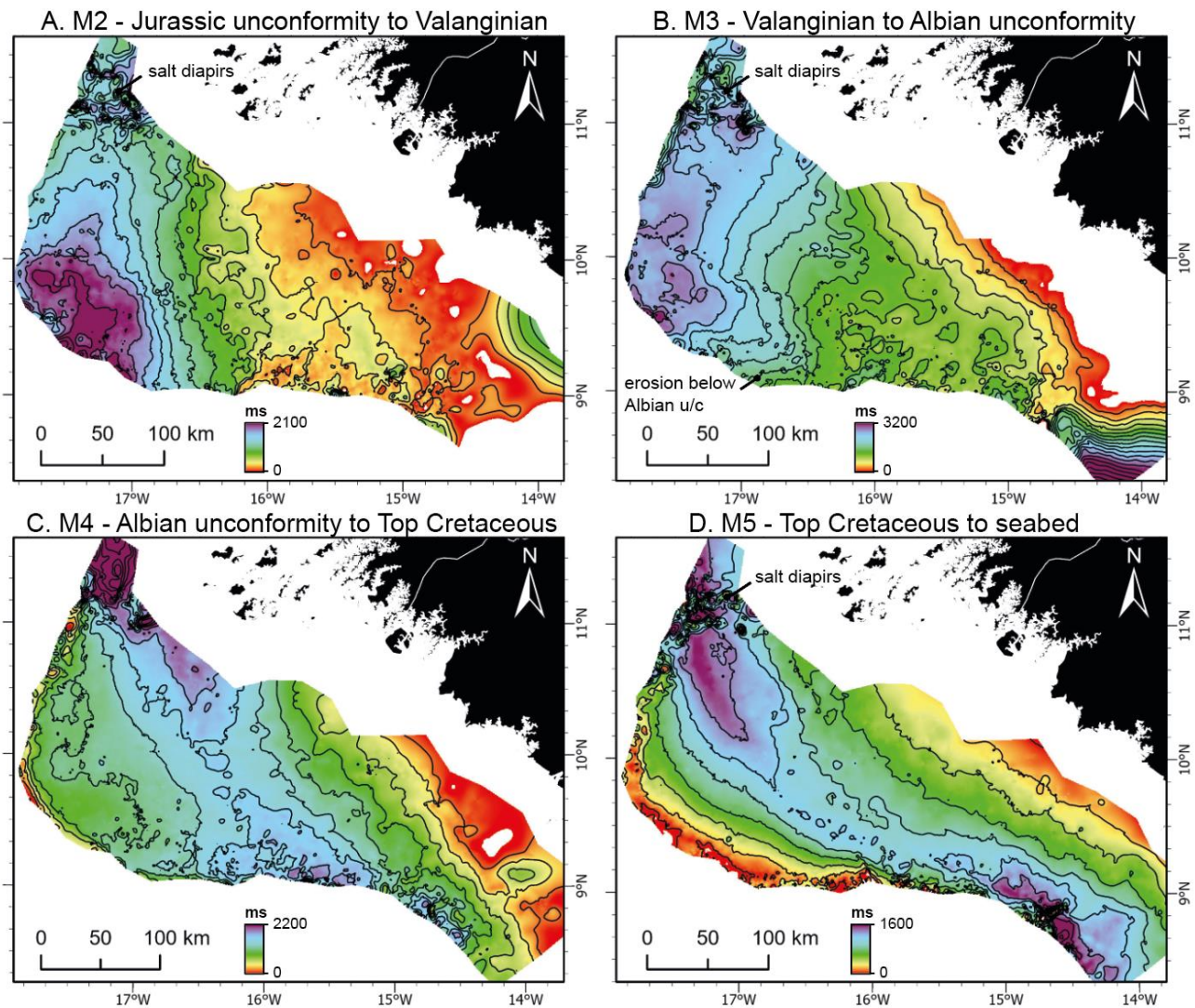


Figure 5. Isochore maps of Megasequences M2-M5 showing the depositional trends within these units, reflecting change in sedimentation pattern as the Guinea margin evolved from the Jurassic to the Cenozoic, before, during and after the opening of the EAG. Contour interval for all maps is 150 ms (milliseconds TWT).

5 (A) M2 consists of carbonate platform facies, with the thickest depocenter on the west of the plateau. This area likely experienced rapid thermal subsidence during this time. (B) M3 consists of clastic sediments derived from both the African margin and possible also the conjugate margin in south America before the opening of the EAG. The sequence is thinner on the southwest, near the GFZ, where the Albian unconformity is most pronounced. (C) M4 consists of clastic marine sediments, with a depocentre across the central plateau, with prograding clinoform systems coming from the African margin.

10 (D) M5 also has a NW – SE depocenter outboard of the contemporaneous shelf edge (Fig. 1), with the thickest areas corresponding to a Mass Transport Complex (Fig. 9).

3.3 Megasequence 3 (M3) – Early Cretaceous syn-transform sequence

The Early Cretaceous syn-transform sequence (M3) is defined by the VG reflector at the base and the regional Albian unconformity (AU) at the top (Figs. 2-4), with a thickness of ~0.5 s to a maximum of 2 s TWT. Three seismic units – SU3, SU4 and SU5 - were mapped within the M3 (Figs. 2-4). These seismic units consist of discrete packages of clinoforms characterised by parallel, oblique to sigmoidal configuration with gentle seaward-dipping, low to moderate amplitude reflections. The internal reflectors are dipping low-to-medium amplitude, discontinuous, wavy and parallel, while toplap and downlap stratal termination characterise the internal architecture. Overall, they show gradual lateral facies change from high-amplitude, continuous parallel to divergent, sub-horizontal reflectors to the west, to moderate-to-low-amplitude discontinuous reflectors to the east.

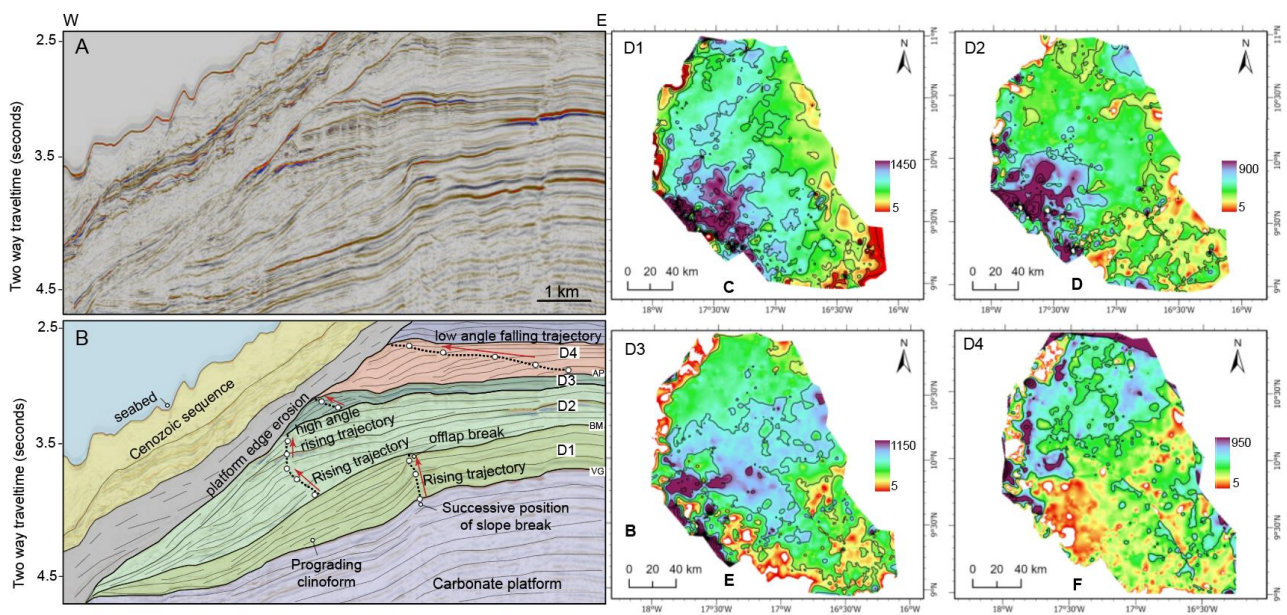


Figure 6. Inset from Figure 5A, showing the Early Cretaceous deltaic complexes of M3, (SU3 – SU5) marked by four clinoform shelf edge systems, or deltaic units. This represents the onset of significant clastic sedimentation into the margin, shutting off the underlying Central Atlantic post-rift carbonate factory. C-F: Isochore maps (TWT, ms) of individual deltaic unit showing the depocenter shift with time.

Four distinct shelf-edge clinoform systems, or delta systems (D1 - D4), were mapped in the M3 sequence, between the VG and AU horizons. These are separated by flooding surfaces, which represent transgressive events between each of the regressive clinoform packages (Figs. 6). D1 is characterised by a well-developed clinoform package with a height (offlap break to downlap) of ~ 450 ms TWT (Fig. 7A). The shelf edge trajectory of D1 exhibits a positive, high-angle rising trend. D2 and D3 were mapped within the SU4 unit bounded by the Barremian (BM) and Aptian (AP) horizons. D2 has a height of ~ 340 ms twt and shows clinoform building out further basinward relative to D1 with the shelf edge showing a continuous rising low-angle trajectory. Overlying D2 is an aggrading, slightly backstepping clinoform unit, D3, that is characterised by a clinoform relief of ~120 ms TWT. D4 was mapped between the Top Aptian and the Albian unconformity.

The thickness maps of the four clinoform systems (D1 - D4, Fig. 6B-F) show a spatial change in sediment accumulation through time. D1-3 have discrete depocenters in the southwest, whereas D4 is located further north along the western margin of the Guinea Plateau.

5 The AU unconformity which forms the top of the M3 is a prominent erosional unconformity, with the greatest amount of erosion occurring in the southwest of the Guinea Plateau (Fig. 3). In this area, all SU5 sequences and the upper part of the SU4 sequence are missing, corresponding to around 420 ms (~ 500 m) of erosion. This unconformity separates the extensively faulted Early Cretaceous syn-transform sequence from the overlying flat, mainly undeformed, Upper Cretaceous to Cenozoic sediments. The extensional faults in the M3 megasequence locally show evidence of a steep lower 'stem' and concave-up top, suggesting that these are
10 strike-slip faults. Although the orientation is not clear from our 2D datasets, other studies of smaller 3D surveys in this region show that these are oriented NW-SE (Olyphant et al., 2017, Nicholson et al., In review). These faults increase in density and amount of displacement towards the SW of the Plateau, where the erosion is also greatest.

15 **3.4 Megasequence 4 (M4) – Upper Cretaceous post-transform sequence**

The Upper Cretaceous post-transform sequence (M4) defines the interval bounded by two regional unconformities – the AU reflector at the base and top Cretaceous (K) reflector at the top (Figs. 2-4, 7). This unit consists of a series of undeformed sequences that are deposited directly above the faulted and eroded M3 megasequence. The base of M4 corresponds to a major transgressive event in the SU6 unit, with internal
20 reflections progressively onlapping the base AU reflector (Figs. 2-4). SU6, mapped across the Guinea Terrace and on the Guinea Plateau, has a distinctive seismic facies, characterised by very high-amplitude, laterally continuous reflections and gradually increases in thickness, by up to ~ 300 ms TWT, towards the southeast, (Fig. 8; See Supplementary Material A6 for individual isochore maps). Four seismic units – SU7, SU8, SU9 and SU10, with a total thickness of ~1km, were mapped above the SU6 unit, separated by prominent erosional
25 unconformities or flooding surfaces (Fig. 2). These seismic units consist of low- to moderate-amplitude, parallel to sub-parallel, laterally continuous reflector correlated across the eastern Guinea Terrace and plateau to the Sabu-1 and GU2B-1 wells. In the western Guinea Terrace, these seismic units have distinct sigmoidal geometries with toplapping and downlapping terminations, that we interpret as clinoform systems (Fig. 7). These clinoform systems are in some cases associated with mass transport deposits (MTDs), with three MTDs
30 mapped in this sequence (Figs. 7 and 8). Individual MTDs extend across an area of 1000-9000 km², and they typically underlie individual regressive, clinoform packages.

This sequence consists of four individual transgressive-regressive sequences above the SU6 unit (Figs. 7 and 8). The K reflector at the top of M4 was mapped and interpreted across the entire margin as an erosional unconformity. It is characterised by high-amplitude, discontinuous reflections on the Guinea Terrace with a
35 change in reflection character from low to moderate amplitude on the shallow Guinea Plateau (Figs. 2-4). A

thickness map of the AU reflector to the K reflector indicates a depocenter that followed a northwest to southeast trend. (Fig. 5C) in the centre of the plateau, where the individual clinof orm systems are thickest.

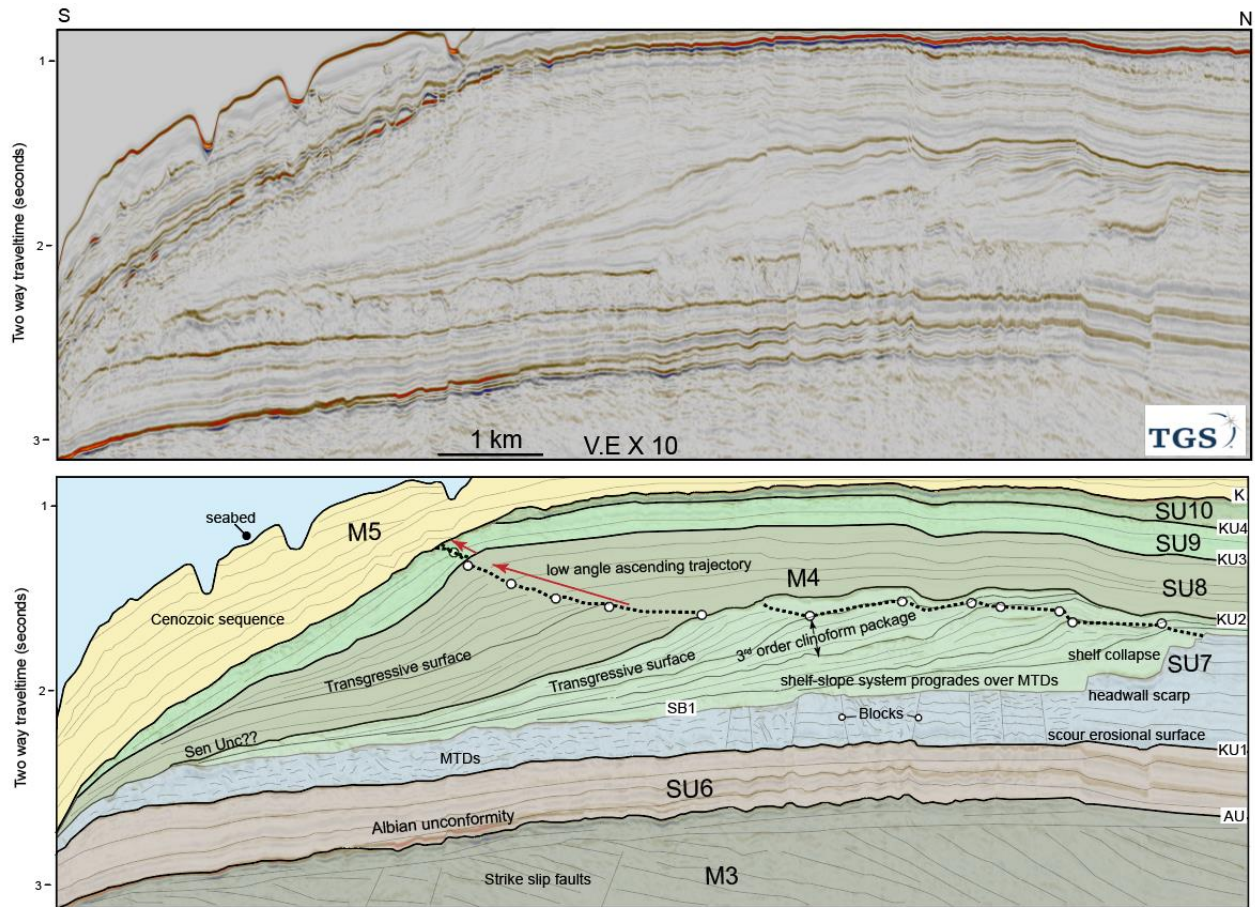


Figure 7. Upper Cretaceous sedimentary sequence including the SU6 early Albian - Cenomanian/Turonian transgressive event and black shale deposit over thin carbonate interval (M4, SU6), late Cretaceous mass transport deposit (SU7) and a series of transgressive – regressive cycle in SU7-SU10

Towards the SE of the margin, the SU6 reflectors progressively onlap a structural high at the northern edge of the GFZ, while the SU7 to SU10 units prograde over the crest of this structure (Fig. 4). This structural feature, that we refer to as the Guinea Marginal Ridge (GMR), forms at the southern plateau margin, just inboard of the Guinea Fracture Zone. It is a near-symmetric ridge with steep flanks and a total elevation of >1 s TWT (>1 km) at the AU reflector and below. Internally, it is characterised by low amplitude, discontinuous reflections, likely due to the difficulty in processing the steeply dipping stratigraphy in this structure. The orientation of the ridge itself is difficult to tell because of the limited seismic coverage in this area, but it is likely to be parallel to or oblique to the GFZ. To the south, an ~20 km zone of rotated and deformed fault blocks occurs between the ridge and the GFZ. This faulted sequence is onlapped by seismic reflectors of M4 in the deeper basin of the Equatorial Atlantic.

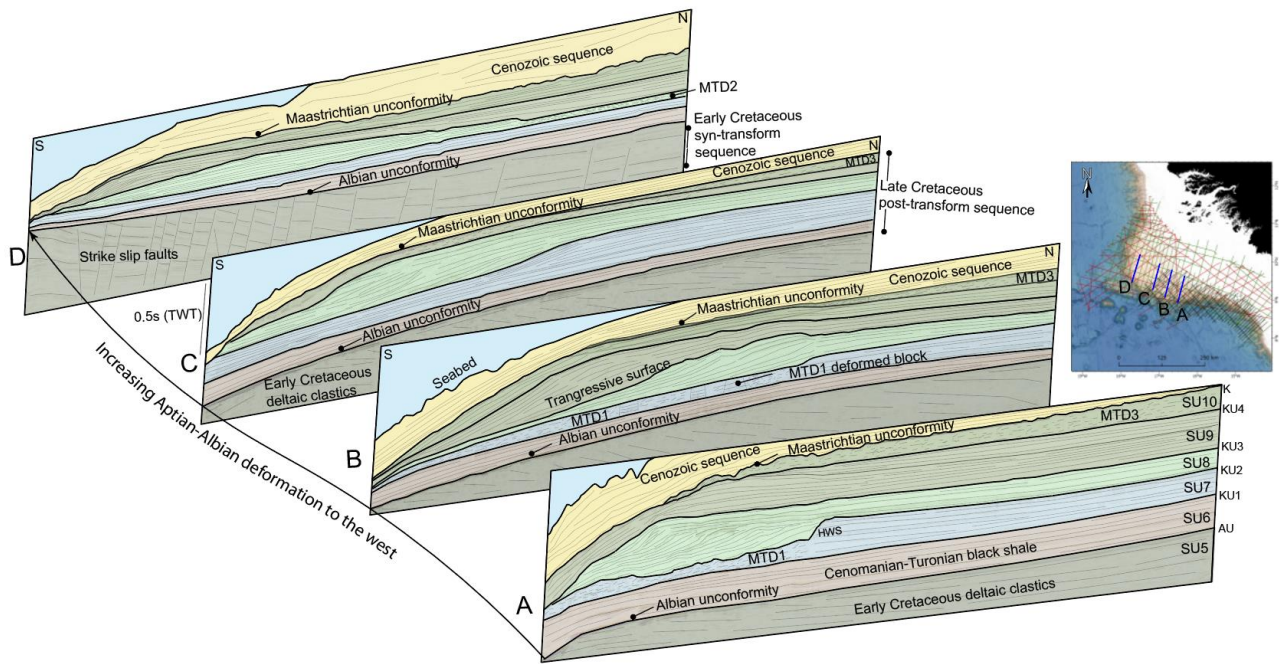


Figure 8. Fence diagram of four regional seismic lines running from NNE – SSW showing the depositional trend in the Upper Cretaceous, including the transgressive – regressive cycle and MTDs. MTDs 1 – 3 are stratigraphically younger towards the north while the intensity of the deformation increases to the NW. Seismic line locations are shown on the inset figure.

3.5 Megasequence 5 (M5) – Cenozoic post transform sequence

The M5 sequence is confined between the K reflector at the base and the present-day seabed (SB reflector) (Figs. 2-4). This sequence progressively thins to the west, with a maximum thickness of ~1100 m on the northwestern Guinea Plateau reducing to less than 500 m across most of the Guinea Terrace (Fig. 5 D). There is only a very thin sedimentary cover above the southern plateau margin, including the GMR (Fig. 4). Five seismic units (SU11 – SU15) bounded by six seismic stratigraphic surfaces were mapped within this interval (Fig. 9). The seismic reflections in this sequence are characterised by low-amplitude, continuous parallel reflections in the Paleogene, and moderate amplitude, chaotic reflections in the Oligocene-Recent.

On the outer Guinea Terrace, a large number of tightly-spaced, small-offset extensional faults are confined between the K and Middle Eocene (ME) horizon, where this unit (SU11-12) has a maximum thickness of over 300 m. These are consistent with polygonal faults that typically form in biosiliceous sediments. A thick carbonate sequence is recorded in the Paleocene – Eocene interval in both the GU2B-1 and Sabu-1 wells in the southeastern part of the basin, consisting of ~350 m of limestone and dolostone interbedded in thin calcareous mudstone (Fig. 2).

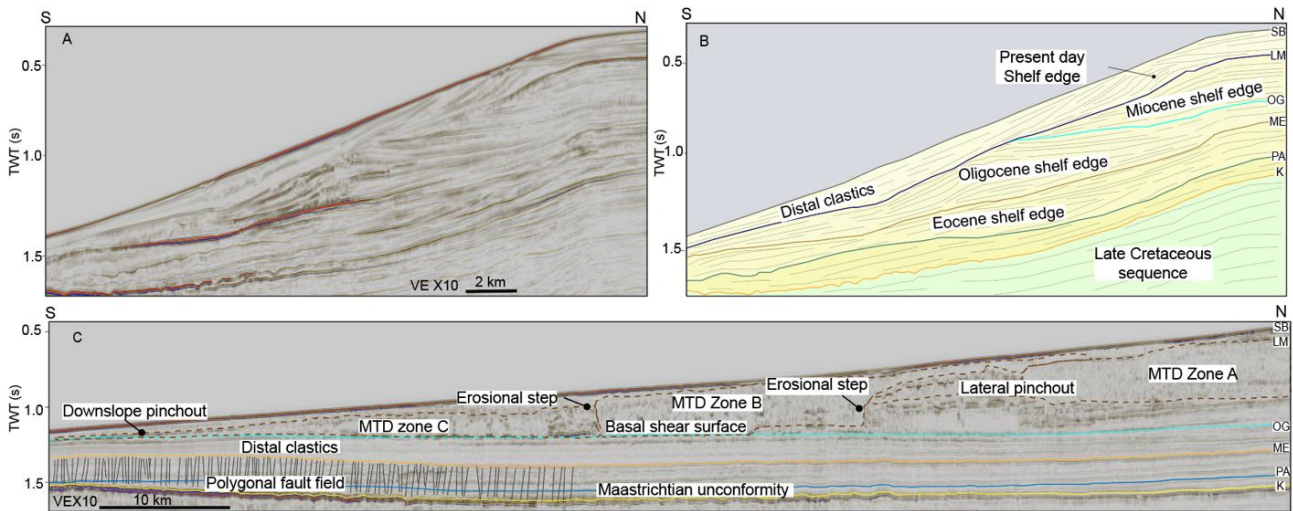


Figure 9. A: Seismic profile showing the main transgressive–regressive cycle in the Cenozoic at the plateau margin. B: Seismic profile on the Guinea Terrace showing Cenozoic sequence including mass transport complex (MTC) deposited on a stable low-angle slope and a Paleogene polygonal fault field indicating biosiliceous sedimentation.

5

The overlying units SU13 - 15, are largely unaffected by polygonal faults, suggesting that the lithology of this unit is different, possibly with more terrigenous (clastic) sediment input. Above this, the shallower units are dominated by a large-volume mass transport complex (MTC) of the SU14 – SU15 units (between the OG and SB reflectors, Fig. 9). This MTC, deposited on a very low-angle slope, is characterised by acoustically chaotic, discontinuous and mostly deformed internal reflections. The thickness of this complex varies between ~ 75-450 m, with the MTC covering a total surface area of 16,264 km². It is likely that this MTC consists of several individual MTDs, each representing individual submarine landslide events. The basal shear surface of this MTC coincides with the Oligocene (OG) reflector, at least in the SW of the Guinea Terrace (Fig. 9).

10

15 3.6 The Guinea Plateau sediment budget

Sediment accumulation rates were calculated for individual seismic units (SU 3 - 15), with average rates calculated for each megasequence (M3 - M5) (Fig. 10). Sedimentation accumulation rates were not calculated for the M2 megasequence, which is assumed to be dominated by carbonates. The M3 syn-transform megasequence between the Albian unconformity (AU reflector) and the Valanginian (VG reflector) has the highest sediment accumulation rate in the Guinea Plateau. A total of ~72k km³ of sediment was deposited during this interval with a sediment accumulation rate averaging 41 m/Myr. An estimated ~57k km³ of sediment was deposited during the post transform (M4) sequence, between the Maastrichtian and Albian unconformities at an average rate of 30 m/Myr, around 25% lower than the average for M3. Sediment accumulation rates during M4 are characterized by significant fluctuation in the sediment volume across the individual seismic units comprising this sequence, with the maximum sedimentation rate of the AU to K sequence recorded between the KU3 and KU4 unit (49 m/Myr). The volume of accumulated sediment in the Cenozoic M5 post-transform

25

sequence is substantially lower than for M3 and M4, with an average rate of only ~10 m/Myr. The variation for individual seismic units is also substantially lower here, with values consistently less than 14 m/Myr.

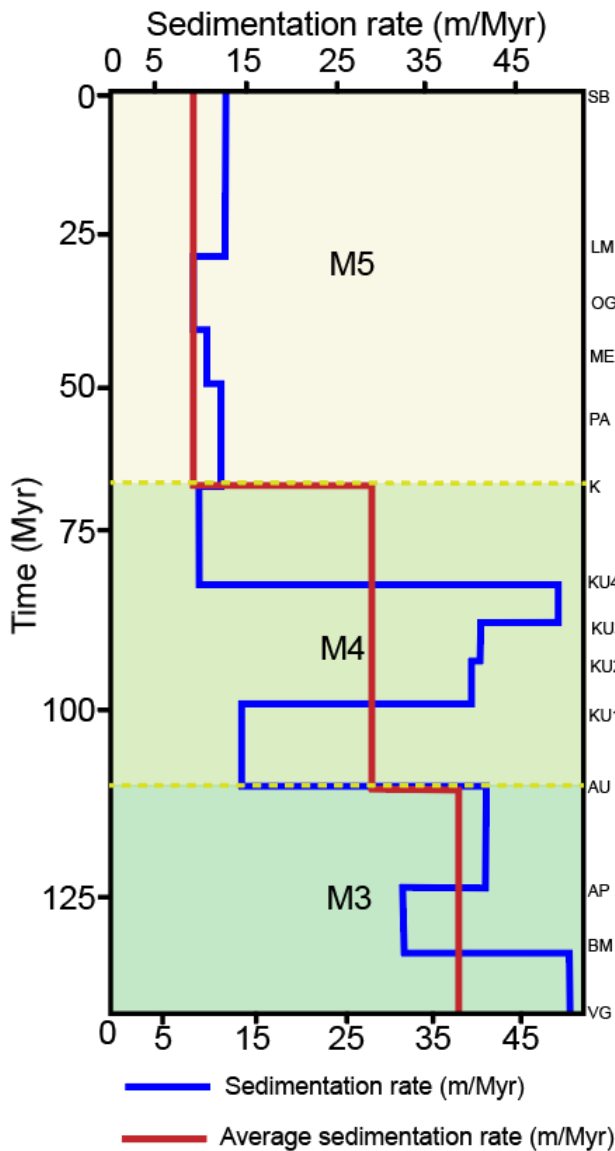


Figure 10. A: Sediment accumulation rates for individual seismic unit (SU, blue line) and average rates for megasequences M3-M5. The K (Top Cretaceous – 66 Ma) and AU (Albian unconformity, ~110 Ma) are regional unconformities that are easily correlated across the plateau, with greater uncertainty over the ages of the other SU boundaries. Thus, the sedimentation rate for the megasequences have less uncertainty than those for individual SUs. M2 was not calculated as this unit is dominated by carbonates, which are not part of the terrestrial sediment budget. Additional data on the velocity model and porosity correction are shown in Supplementary Material A3

3.7 Organic Geochemistry – GU2B-1 and Sabu-1 Wells

The TOC concentration of samples from the GU2B-1 well range from 0.11 to 2.92 %, with a mean value of 0.88% (Fig. 11A) and elevated concentrations within the Cretaceous interval. Samples from the Cenomanian – Turonian period, a 90 m thick deposit of brown to dark grey shale, have the highest TOC values, up to 2.92 %, with an average of 1.5 %. HI and OI from Rock Eval analyses, applied to assess kerogen type and quality, show HI values ranging from 22 - 461 mg/g TOC and a wide range of OI values from 62 – 277 mg/g. Low HI (22 – 118 mg/g TOC and average of 70 mg/g TOC) is recorded within the Cenomanian-Coniacian interval with the elevated TOC. Independent vitrinite reflectance (VR) value ranges from 0.5 -2 Ro across the Cenomanian - Turonian section. The high VR value may however indicate reworked vitrinite. A modified van Krevelen plot of HI and OI parameters confirms a dominance of kerogen type III throughout the study section of GU2B-1 (Fig. 11B).

The Sabu-1 well also shows similar concentrations of TOC in the sixty-eight samples, with values ranging from 0.11 – 2.17 %, averaging at 0.84 %. The depth plot of Sabu-1 TOC shows less pronounced variability compared to GU2B-1 but still has a cluster of scattered elevated values between the Cenomanian - Campanian interval, including a 40 m thick Top Turonian interval of light grey to dark/black shale (Fig. 2). TOC values range from 0.64 – 1.36 % with an average of 0.95 %. (Fig. 11B). Corresponding HI values range from 76 – 280 mg/g/TOC while the OI is relatively low, with values ranging from 22 – 107 mg/g. The Tmax profile shows values between ~ 430 and 440 °C across a ~1.5 km depth section, suggesting early mature burial conditions. At this level of thermal maturation, we cannot exclude some alteration of the primary organic matter, shifting HI to lower levels and impacting kerogen typing. The HI and OI plot identifies kerogen Type III as the dominant organic facies, however with a wide range of oxygen-bound organic matter. A potential enhanced marine component leading to kerogen Type III/II for some of the Cenozoic sediments is indicated based on the available geochemical information.

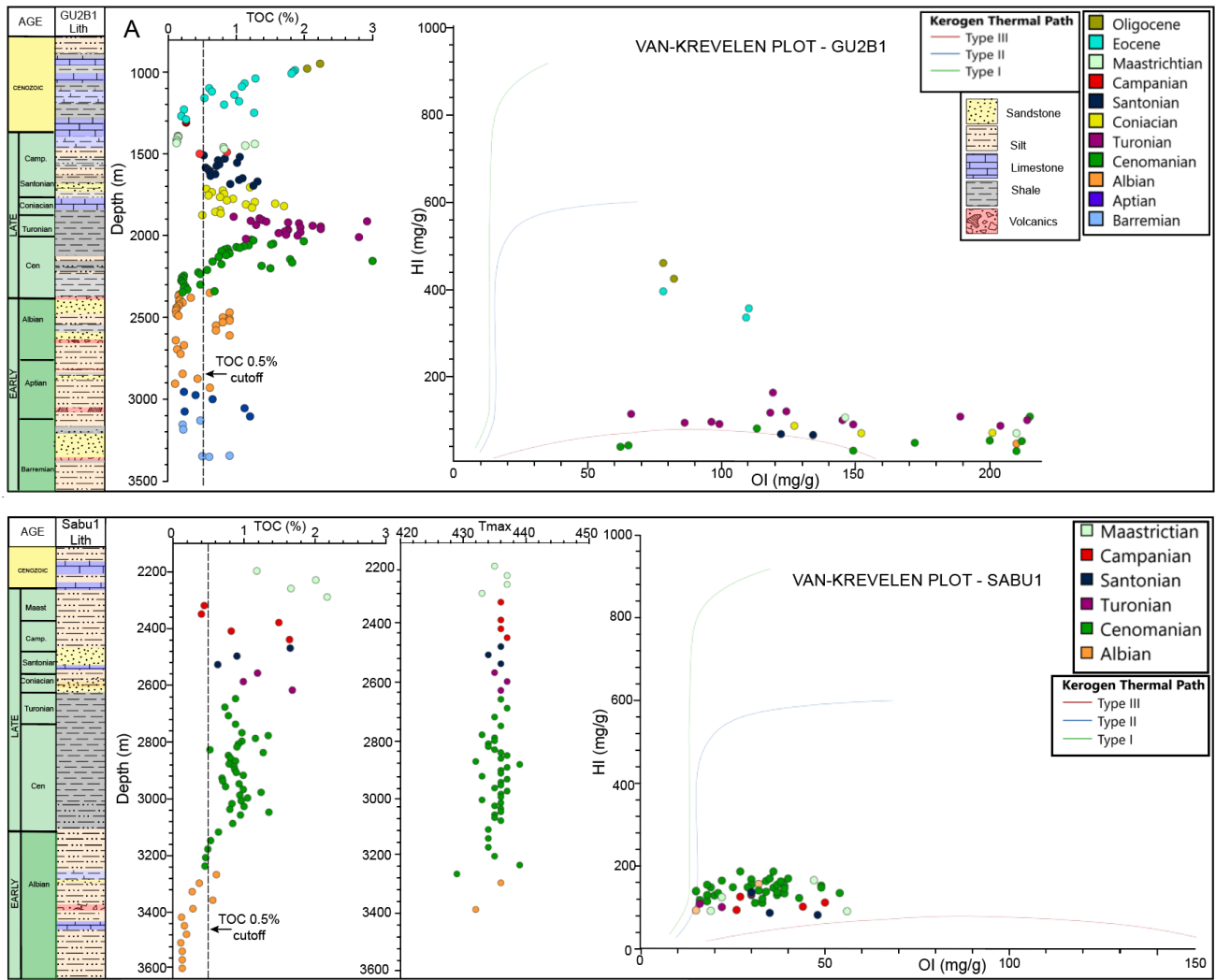


Figure 11. Organic geochemical analysis for (A) GU2B-1 and (B) Sabu-1 wells. Total Organic Carbon (TOC) shown plotted against depth, with T_{max} values shown for Sabu-1 (no corresponding data for GU2B-1). For kerogen type and T_{max} thermal maturity assessment we exclude samples with TOC concentrations below 0.5%. Van Krevelen plots for both cores show that most data from the Cretaceous sediments correspond to Type III kerogen, indicating a terrestrial or reworked origin for organic matter at these sites. This assessment does not include potential overprint from upper oil window thermal degradation of the organic matter.

4. DISCUSSION

10 4.1 Tectonic and sedimentary evolution of Guinea Plateau

The seismic stratigraphic interpretation of the 2D regional seismic lines (Figs. 2-4) allows for a synthesis of the structural and stratigraphic events on the Guinean Margin from the Jurassic to Recent. These events are captured in megasequences (M1 – M5) that divide the basin into (i) a Jurassic Central Atlantic syn-rift sequence, (ii) a Jurassic to Early Cretaceous Central Atlantic post-rift sequence, (iii) a late Early Cretaceous syn-transform sequence, (iv) an Upper Cretaceous post transform sequence and (v) a Cenozoic post transform sequence. In this section, we discuss the primary controls on the deposition of these megasequences.

Central Atlantic syn-rift phase (M1)

M1 consists of the Jurassic sequence that lies directly above older Palaeozoic pre-rift sediments and crystalline basement. It represents the syn-rift phase of the Central Atlantic breakup event. This sequence likely consists of volcanics, salt and clastic sediments (Figs. 2-4) deposited in a series of north-to-south trending basins (grabens and half-grabens) with a similar sedimentary evolution to other sub-basins within the wider MSGBC basin (Frizon De Lamotte et al., 2015; Leleu & Hartley, 2010). These basins developed along the Central and North Atlantic conjugate margins of NW Africa and North America, during the Late Triassic – Earliest Jurassic rift (Withjack & Schlische, 2005). Igneous and volcanic materials interbedded in the M1 unit are derived from Triassic magma (the CAMP large igneous province) related to the Central Atlantic rift event (Leleu & Hartley, 2010; Marzoli et al., 1999). These volcanics are also seen as SDRs that formed at the continent-ocean transition during the rift (Figs. 2-4, 12A). Evidence of volcanism and SDR development is also observed on the conjugate margin in South America (Casson et al., 2021; Reuber et al., 2016).

Salt deposition during the Late Triassic and Early Jurassic suggests that this region was affected by restricted marine conditions and an arid climate, both in Guinea and across the wider margin (Tari et al., 2003). On the Guinea Plateau, a salt basin only formed locally in the NW area, offshore Guinea Bissau (Fig. 13). Syn-rift sedimentation in the Central Atlantic segment stopped during Early Jurassic (Leleu et al., 2016), which likely correlates to the Lower Jurassic regional breakup unconformity (JU reflector, Figs. 2-4, 12) that tops M1, with its erosive nature indicating subaerial exposure of the Guinea Plateau.

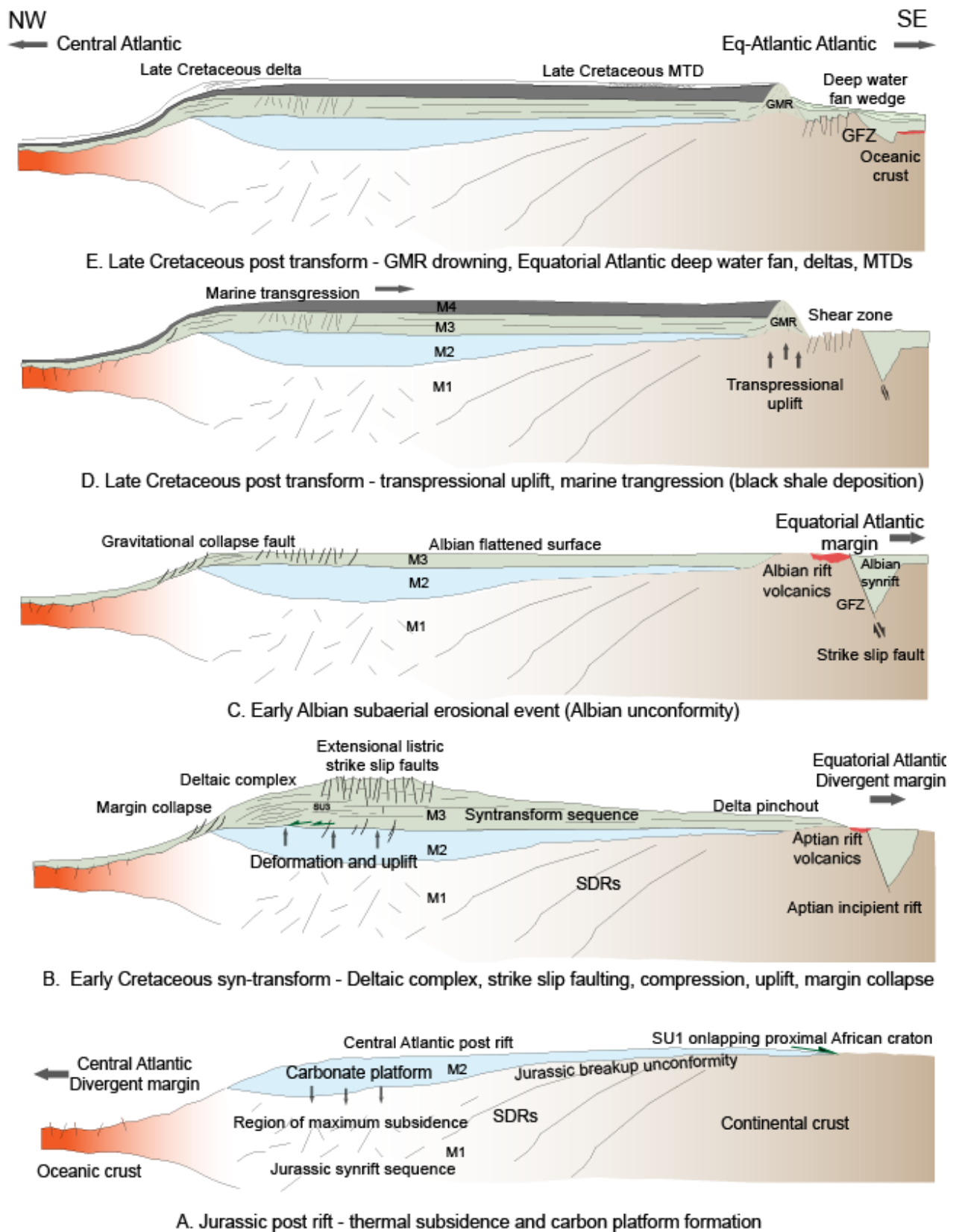


Figure 12. Schematic cartoon of the Guinea Plateau evolution from the Jurassic to Late Cretaceous, encompassing the opening of the EAG, between C and D. A. Jurassic post-rift after the Central Atlantic rifting event - thermal subsidence and carbon platform formation. B. Early Cretaceous (Valanginian to Albian) syn-

transform phase showing the deltaic complex (D1 – D4), strike slip faulting, compression, uplift, margin collapse. Rift initiation in the Aptian and beginning of Equatorial Atlantic opening. C. Peneplained surface resulting from the subaerial erosional event in the Early Albian. D. Late Cretaceous post transform - transpressional uplift (GMR), marine transgression (black shale deposition). E. Late Cretaceous post transform - GMR drowning, marine deposition across the Guinea Plateau and adjacent areas.

5

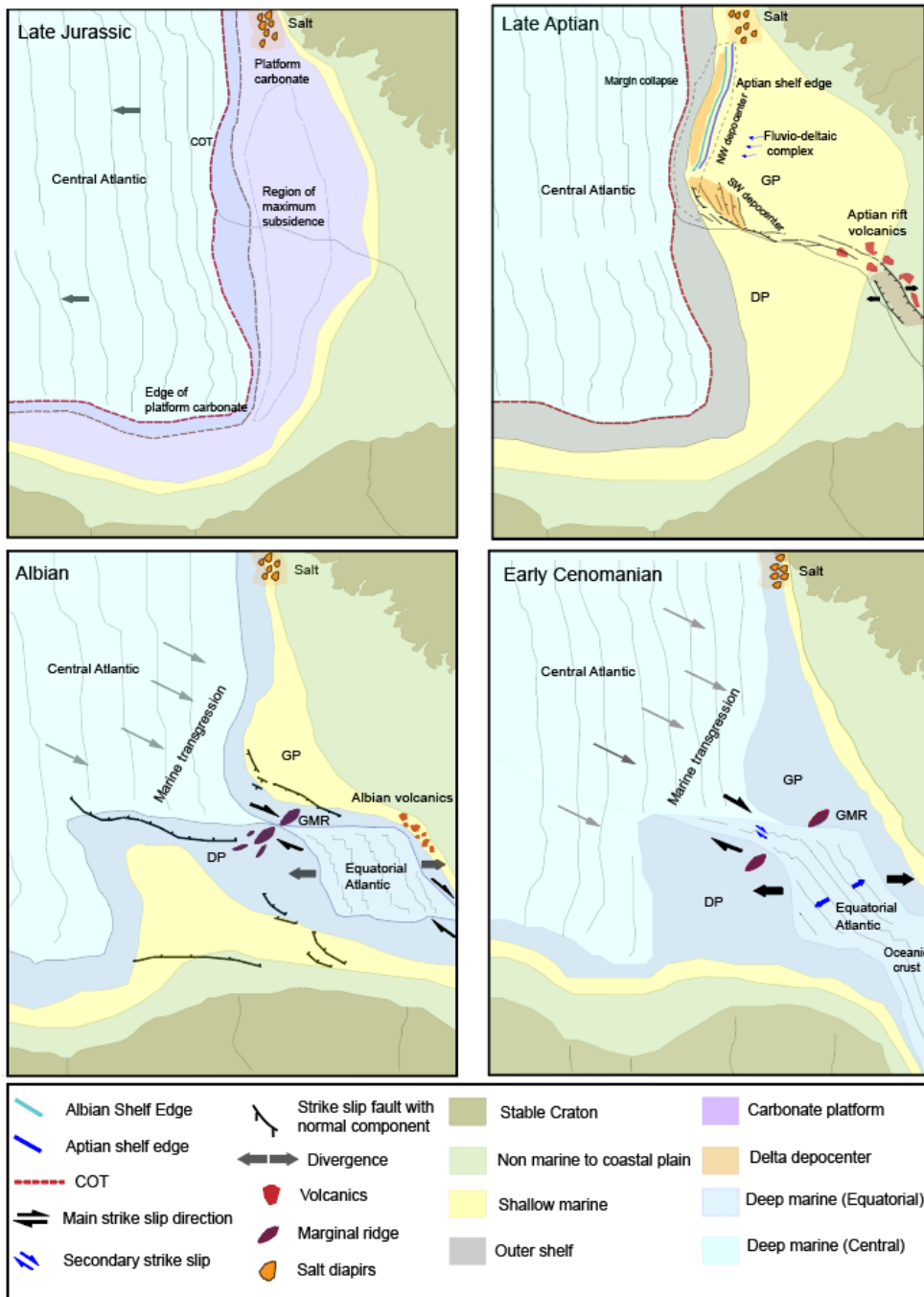


Figure 13. Palaeogeographic maps for the discrete time periods before, during and after the opening of the EAG.

10

Carbonate platform growth during the Jurassic to early Cretaceous post-rift phase (M2)

Directly overlying the Central Atlantic breakup unconformity (JU reflector) are the post-rift deposits of M2 (Figs 2-4, 12A) which followed the late Early Jurassic to early Middle Jurassic rift-to-drift transition in the Central Atlantic domain (Biari et al., 2017; Leleu & Hartley, 2010). The seismic facies of M2 is consistent with those observed elsewhere in carbonate platforms (Burgess et al., 2013; Hendry et al., 2021). Subsidence and platform aggradation was greatest in the west of the plateau, above the SDR sequence, where the crust is thinner and thermal subsidence more pronounced. On the Demerara Plateau, the conjugate megasequence is composed of limestone and mudstone of Tithonian age (Casson et al., 2021), which may indicate a carbonate platform extending along the northwest–southeast trend with the Guinea and Demerara margin as its southern end (Fig. 13). Carbonate deposition continued through to the Early Cretaceous, indicating little to no clastic input to the distal plateau during this time.

Clastic sedimentation in the Cretaceous syn-transform phase (M3)

The transition from M2 to M3 corresponds to a major change in seismic facies, that corresponds to the end of carbonate deposition and onset of significant siliciclastic sedimentation, with deltaic deposition from the Valanginian to the early Albian (Figs. 6, 13B). Prior to the breakup of Western Gondwana (Fig. 10), sediments sourced from the conjugate margin in South America may have contributed to the peak sediment accumulation rates of M3 (Fig. 13A). Seismic evidence has shown that the Early Cretaceous deltas in this sequence are likely older than the Aptian (Figs. 2B, 13A, SM A2), contrary to previous interpretations (Dombrowski et al., 2002). This can be seen from the Barremian-Hauterivian (SU3, Figs. 2-4, 6) clinoform systems downlapping against the top Valanginian surface (VG) (Fig. 6) and the presence of siliciclastic materials (sandstone interspersed with mudstones) within the deepest Barremian interval in the GU2B-1 well (Fig. 2B, SM A2). On the Demerara Plateau, similar sedimentation processes occurred during the Hauterivian (Casson et al. (2021), indicating that the onset of deltaic systems on both conjugate plateaus started prior to the Aptian.

The M3 sediments were deposited during an active transtensional regime during the Early Cretaceous (Valanginian to early Albian) continental transform stage (Heine and Brune, 2014). This period is characterised by oblique rifting, segmented by transform faults, and gravity-driven deformation at the western plateau margin (Fig. 12B; Duarte et al, in review), with the intensity of structural deformation increasing towards the south and west of the Guinea margin (Figs. 3, 8). This tectonic forcing, and particularly uplift at the southern plateau margin, may have been responsible for the northward migration of the depocentres of individual deltas during this time (Fig. 6).

The Aptian compressional regime (Marinho et al., 1988) led to the deformation and uplift of the SU3 – SU5 sequence (Figs. 12B). This deformed and uplifted package across the Guinea Plateau was subsequently exposed and eroded resulting in the formation of the Albian Unconformity (Figs. 2-4, 12C) including a peneplained surface across the SW of the Guinea Plateau. On the corresponding Demerara Plateau, the breakup

unconformity is also observed, and is dated as near-base Albian (Casson et al, 2021; Fig. 14). Evidence of subaerial erosion is documented there, with reddish oxidised sand below the unconformity in offshore wells.

Sediment routing during the Late Cretaceous post-transform phase (M4)

5 The beginning of the M4 sequence on the Guinea margin is marked by the deposition of carbonates and mudstones (SU6, Fig. 7). These lithologies are inferred based on the similarity of seismic facies between the Guinea Terrace and Demerara conjugate margin, where the sequence includes black shales with up to 20% TOC (Casson et al., 2021). A global early Albian-Turonian transgressive event resulting from eustatic sea level rise (Haq, et al., 2014) resulted in the extensive and widespread flooding of continental margins, including the Guinea margin. This transgressive phase was likely enhanced locally by thermal subsidence following the
10 breakup unconformity of the Equatorial Atlantic, with widespread marine deposition across the study area (Fig. 7, 12D).

Structural deformation continued during the Albian-Cenomanian along the southern margin of the plateau, with the formation of the GMR (Fig. 4). This structural ridge formed as the result of crustal shortening, likely orthogonal to the active shear motion, in an overall transpressional regime when the Guinea Margin was in a
15 transform (post-rift) tectonic setting (Marinho et al., 1988). This feature is overlapped by the Upper Cretaceous sequence (Figs., 4, 14), in particular the Albian-Cenomanian, which shows that the structure clearly post-dates the early Albian break-up unconformity, and that the structure likely persisted as a prominent bathymetric feature until at least the Turonian. On the Demerara Plateau, Greenroyd et al. (2008) interpreted a similar non-tilted, relatively high relief ridge with steep edges located at the northern margin of the plateau (Fig. 14). Both
20 structures formed after the syn-rift stage, during the transform margin stage, as observed at other transform margins (Basile et al, 2015).

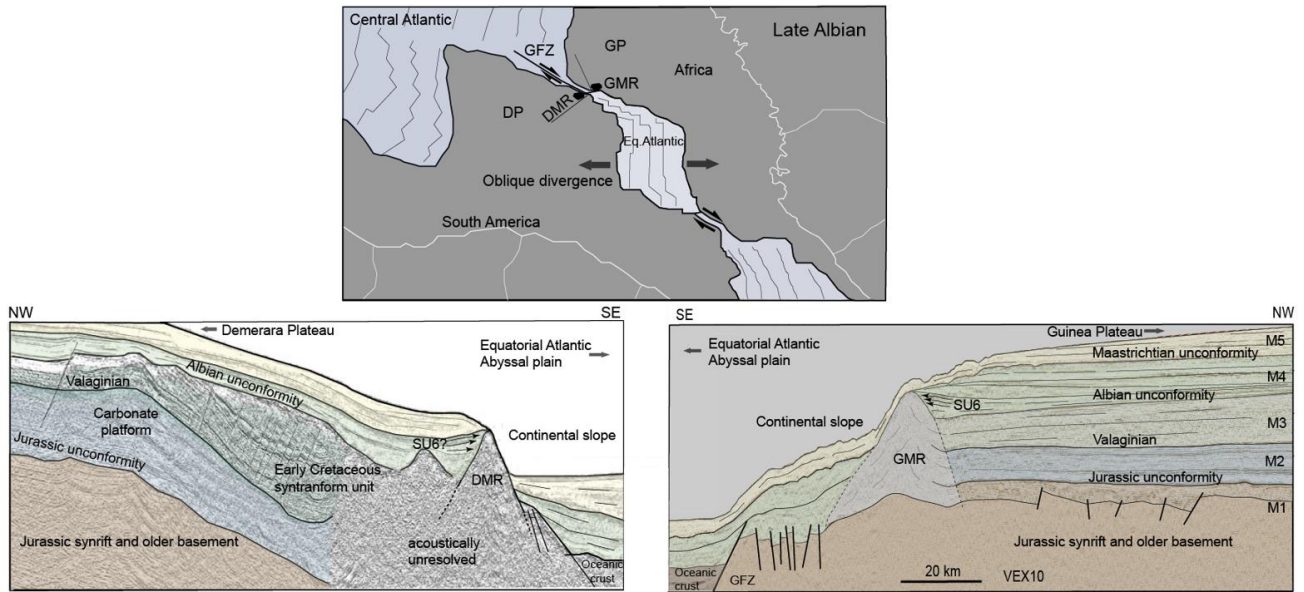


Figure 14. (A) Tectonic reconstruction of the emerging Equatorial Atlantic Gateway during the late Early Albian, based on the Geognostics Earth Model ([Geognostics Earth Model](#)). (B) and (C) are seismic profiles from the Demerara Plateau (Greenroyd et al., 2008) and the Guinea Plateau (this study) showing the presence of marginal ridges on both conjugate margins.

5

Following the end of the early Albian–Turonian transgressive event, increased sedimentation on the Guinea Plateau led to the deposition of units SU7 - SU10, with the depositional system characterised by large MTDs and several transgressive-regressive cycles (Figs. 7, 8). The switch in the Upper Cretaceous depocenter and sedimentation pattern to a NW – SE trend (Fig. 6) along with a reduced sedimentation rate (compared to the Early Cretaceous; Fig. 10) suggest a significant change in sediment routing to the Guinea Plateau. Any sediment routing from the conjugate South American margin would have been cut off, but there is also potential for a significant drainage reorganization from the African continent to the east (Mourlot et al. (2018). Late Cretaceous sediment routing and deposition may also have been influenced by regional uplift in the north and west of Africa at ~94 – 84 Ma, associated with the collision of the African and European plates (Guiraud & Bosworth, 1997), and may be a driver of the contemporaneous slope failure and MTCs on the Guinea Plateau (Figs. 7, 8). The top of the post-transform sequence, marked by the K-Pg boundary, is interpreted to be the result of widespread liquefaction and ejecta due to a local hypervelocity impact event (Nicholson et al., 2022, Nicholson et al., in review)..

10

15

Cenozoic subsidence and sedimentation on the Guinea Terrace (M5)

Post-transform sedimentation continued following the K-Pg boundary (K reflector), with the deposition of Paleogene to Recent sediments (Figs. 2-4). Thin layers (15 -20 ms) of Paleocene carbonates, recorded in the GU-2B-1 and Sabu-1 wells (Figs. 2c, Supplementary Material A2), onlap the K-reflector, and formed because of regional subsidence following the Maastrichtian unconformity (Olyphant et al, 2017). Seismic evidence suggests that the overlying sediments are mostly fine-grained distal clastics deposited on the upper to lower

20

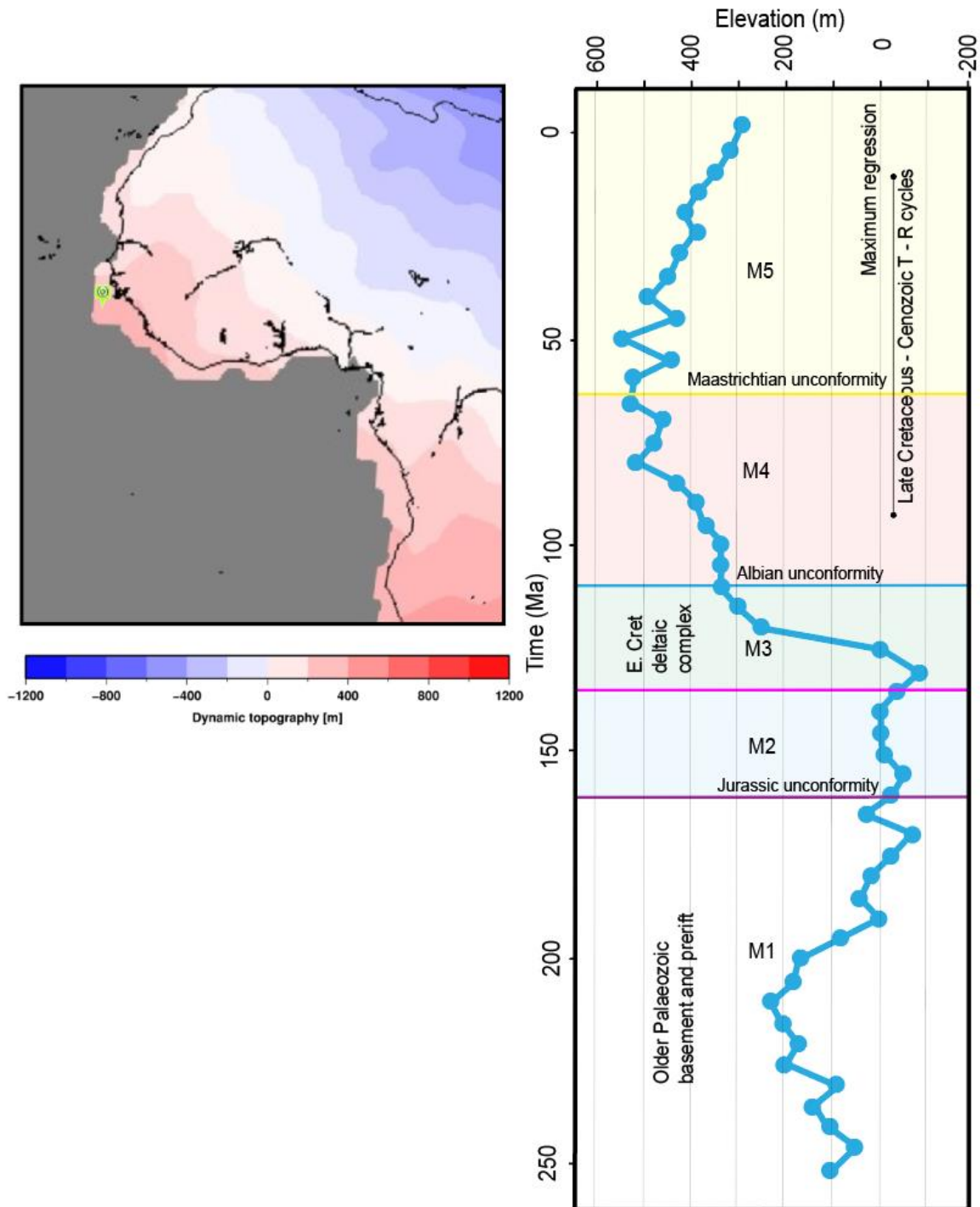
slope across the Guinea Terrace (Figs. 2-4, 9). A large, laterally extensive, polygonal fault field in the SU12 unit of the NW Guinea margin slope domain (Figs. 4, 9) indicates biosiliceous sediments, with polygonal faults forming due to volume loss during dewatering and compaction (Cartwright, 1993; Xia et al., 2022). Predominantly siliceous sediments also suggest a lack of clastic input during that time, consistent with the observations of carbonates in the wells. This sequence coincides with a major marine transgression across West Africa, with the shoreline several hundred kilometers to the east of the present day (Chardon et al., 2016).

The Oligocene-Recent stratigraphy of the Guinea Terrace is also characterized by very low rates of sedimentation, with limited clastic deposition except for a large mass transport complex (MTC) (Fig. 5D, 9C). The individual MTDs within this complex are deeply erosive, indicating high flow rates, despite forming on a very low slope angle slope, in a ramp setting. These events may possibly be linked with rejuvenation of terrestrial sediment flux because of uplift in the hinterland, particularly the Hoggar swell (Liégeois et al., 1990). The topographic relief formed by the Hoggar hot spot played a significant role in the reorganization and stabilization of drainage basins by the late early Oligocene period and extending to the end of the Eocene (Chardon et al., 2016)). This stabilization facilitated the connection between hinterland denudation and clastic sedimentation to the coast. Rapid weathering, erosion and sediment transport leading to high clastic sediment flux during this period could also have been driven by the hothouse climatic conditions during the Eocene (Tierney et al., 2022). However, since this time, the generation of accommodation space on the plateau clearly exceed the sediment flux to the basin as shown from the continued low sediment accumulation rates on the Guinea Terrace in particular (Fig. 10).

4.2 Controls on transgressive-regressive cycles on the Guinea margin

The presence of transgressive-regressive (T-R) cycles in the Guinea margin, both in the Upper Cretaceous and early Cenozoic periods, suggests that there have been significant relative sea level changes or changes in sediment supply at higher time frequencies than the 1st order (~25-65 My) megasequences. For example, there are 5 prominent T-R cycles in the late Albian-Maastrichtian M4 sequence (Fig. 7), with an average duration of <10 My. While these fluctuations in accommodation space or sediment flux may have been driven by a variety of factors, including changes in glacioeustasy (Miller et al., 2003) and plate tectonics (Artoni et al., 2007; Garefalakis and Schlunegger, 2019), dynamic topography is also increasingly recognized to play an important role on stratigraphic architecture at such timescales (Moucha et al., 2008). Regional vertical displacements of the Earth's surface in response to underlying mantle flow (Moucha et al., 2008) result in positive (mantle upwelling) or negative (downwelling) dynamic topography, with sufficient uplift or subsidence to create cyclic depositional sequences (Conrad & Husson, 2009). The recent global dynamic topography of Young et al. (2022) reveals regular ~100 m amplitude fluctuations in the Guinea Plateau region between 95-40 Ma occurring on timescales similar to the Upper Cretaceous to Cenozoic T-R cycles (Fig. 15). Dynamic topography should be considered as a potential driver of these 8-12 My (2nd order) sequences, especially during the post-rift 'passive margin' phase. Continued and pronounced dynamic subsidence from ~40 Ma (Fig. 21) is consistent with the

observation that regressive cycles ceased, the shelf-edge retreated closer to its present position (Fig. 1), and the low Cenozoic sediment accumulation rates across the entire Guinea margin.



5 **Figure 15.** Dynamic topography of the Guinea Plateau, from the model of Young et al. (2022) - [Young's GPlate Model](#). (A) map of the present-day dynamic topography of West Africa, showing the location of the profile in B. (B) Dynamic topography curve since 250 Ma showing major changes in surface uplift, with M1-M5 megasequences superimposed. This model shows major surface uplift during M3, which is truncated by the Albian unconformity. Dynamic topography is at its maximum during M4 and M5, with significant short-term

fluctuations between ~90-40 Ma, corresponding to the T-R cycles of the Upper Cretaceous and Palaeogene. Dynamic topography decreases from around 40 Ma, resulting in subsidence, corresponding to a phase of major transgression during M5.

5 Dynamic topography may also have contributed to the gradual shallowing of the plateau during the Early Cretaceous, and the formation of multiple regressive deltaic sequences near the western plateau margin at this time (Fig. 6). This eventually culminated in the erosional Albian Unconformity (Figs. 2-4, 15-16). However, this phase also corresponds to Equatorial Atlantic rifting and initiation of the continental transform margin between the Guinea and Demerara plateaus (Fig. 16), and it is difficult to deconvolve the dynamic topography and tectonic components of surface uplift.

10 We also show evidence of sequences of shorter duration, within these 2nd order cycles, with at least 5 individual 3rd order sequences evident in SU7, likely corresponding to a time interval of 1-2 My (Fig. 7). Haq et al (2014) documented ~ 40 cycles in the Cretaceous of 1-2 My duration, that likely correspond to these 3rd order cycles (Fig. 16) and may be related to relative sea level changes caused by variations in mid-ocean ridge spreading rates or orbital forcing (Berger et al., 1990.; Royston et al., 2022; Wright et al., 2020)

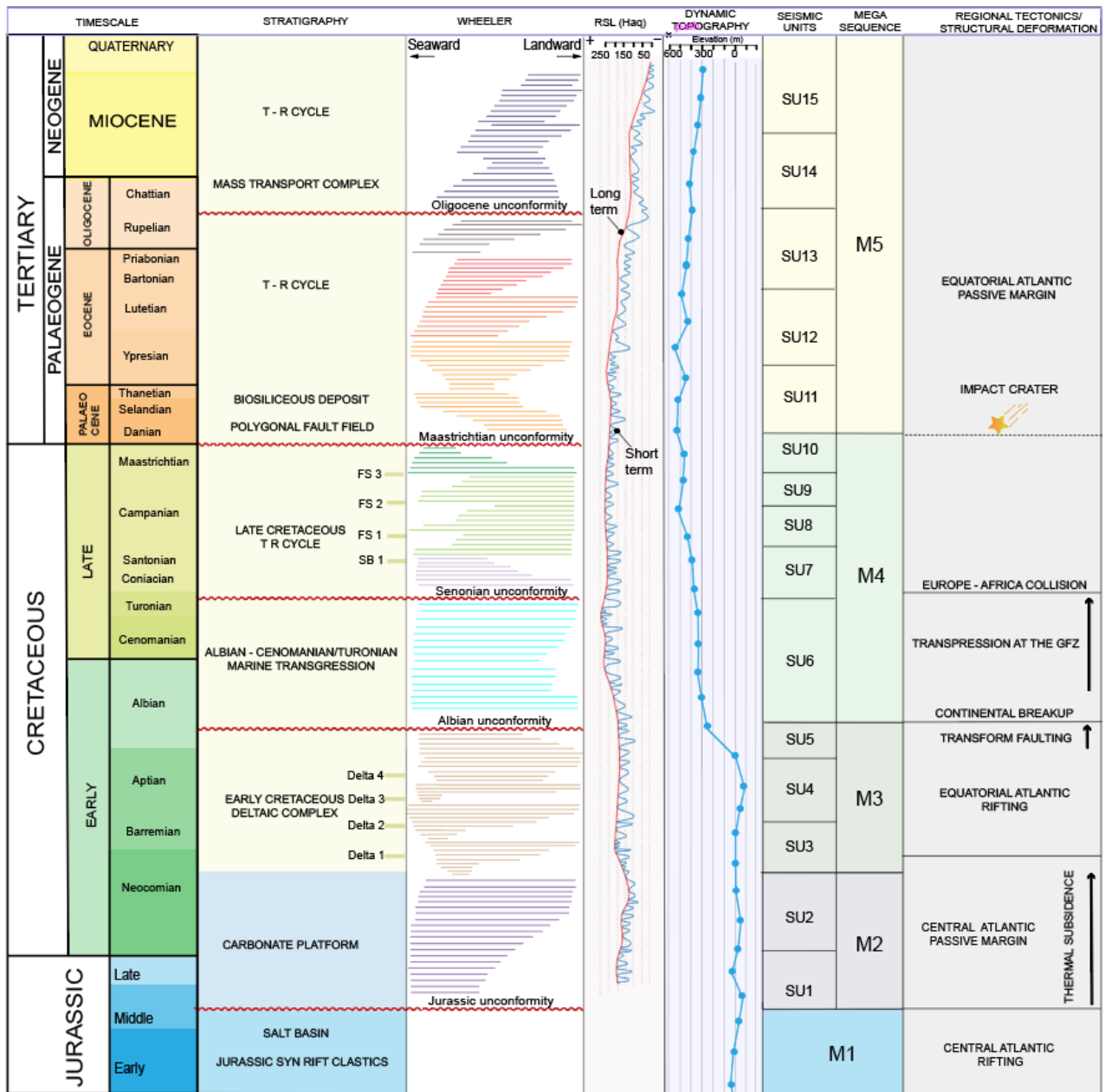


Figure 16. Integrated chronostratigraphic events chart of the Guinea Plateau since the Mid Jurassic.

4.3 Evolution of the EAG and organic carbon burial during OAE2

The sections above describe the long-term (~10-100 My) and medium-term (~5-15 My) controls on the stratigraphic evolution of the Guinea Plateau. We next consider the unique sequence of events defining the critical period of the Cenomanian-Turonian OAE2 in the opening EAG, and the potential relationships for ocean circulation and enhanced organic carbon production and burial.

The breakup (rift-to-drift transition) on the Guinea Plateau was associated with a pronounced erosional unconformity across the Guinea Plateau and Terrace, implying widespread subaerial exposure up to the Early Albian. However, recent geochemical evidence from neodymium isotopes (Dummann et al., 2023) and seismic

stratigraphic observations (Duarte et al., in review) show that there must have been a marine connection already established by the late Aptian-early Albian, during the continental rift and transform phase. The Albian subaerial unconformity noted on the Guinea margin shows that this connection must have been shallow and established along a narrow set of rifts and transform valleys (Duarte et al., in review), with the adjacent areas of the Guinea Plateau and Demerara Plateau subaerially exposed.

The SU6 unit that sits immediately above the Albian breakup unconformity archives the Early Albian-Cenomanian/Turonian marine transgressive event that included the global OAE2. This event saw the widespread deposition of organic-rich black shales (Erbacher et al., 2004; Jarvis et al., 2011; Schlanger et al., 1987; Wagner, 2002), recorded in wells across the North, Central and South Atlantic domains. Consistent with other records, the Guinea Plateau GU2B1 and Sabu-1 lithologies are enriched in organic matter in the critical stratigraphic interval, but it is characterised by type III kerogen for Cretaceous sediments in Sabu-1, suggesting preferential supply and burial of terrestrial and oxidized organic matter from the African continent in a largely oxic depositional environment. These observations show the enhanced deposition of reworked terrestrial organic matter on the Guinea Plateau during peak OAE greenhouse conditions, rather than the marine-derived organic carbon seen at other Central and North Atlantic locations. With the resolution of the geochemical data available we cannot rule out the presence of orbital-scale variations in organic carbon deposition, within terrestrial-oxic (documented here) and more oxygen depleted environments (not yet recovered).

Despite the establishment of a water mass connection between the South and Central Atlantic since the Late Aptian or Albian (Dummann et al., 2023; Murlot et al., 2018, Duarte et al., in review), the structural barrier created by the presence of the transpressive marginal ridge (Fig. 14) on both conjugate margins together with the uplifted/subaerial Guinea and Demerara plateaus may have partially restricted water mass connection through the Equatorial Atlantic Gateway. Despite this restriction, well data from the Guinea Plateau however suggest a persistent oxic environment, at least on the shallow shelf. With the development and widening of the transform valley between the Guinea and Demerara Plateaus (Loncke et al., 2022, Duarte et al., In review), the conjugate ridge became progressively separated and deeper (Fig. 14). As drifting and subsidence continued, leading to the deepening of the gateway and gradual drowning of the ridge, sediments of Coniacian – Santonian age were deposited above the GMR, draping over onto the Equatorial Atlantic domain (Fig. 14). The sedimentary response after this period reflects a gradual transition to more oligotrophic and oxic conditions. This is observed in sediments of the ODP Leg 207 Demerara Rise with Early Campanian glauconitic chinks containing benthic foraminiferal faunas, indicating increased bottom-water oxygenation and low organic matter concentration (Friedrich & Erbacher, 2006). This is the result of a through-going marine connection between the basins of the Central and Southern Atlantic by this time.

5. Conclusion

Over the last 150 Myr, the Guinea margin off tropical West Africa has been shaped by a series of tectonic, geodynamic processes that impacted sediment flux and deposition, and controlled the stratigraphic evolution of the plateau and the Equatorial Atlantic Gateway (EAG) between the South Atlantic and Central Atlantic oceans.

5 The ~25 – 65 Myr scale megasequences interpreted in the Guinea margin are primarily controlled by tectonic processes. The Jurassic syn-rift sequence (M1) consists of clastic sediments, volcanics and salt deposited in a series of restricted marine basins during continental break-up of North America and Africa. The Jurassic to
10 Early Cretaceous Central Atlantic post-rift sequence (M2) was affected by rapid thermal subsidence of the margin and the deposition of a carbonate platform. This was followed by an Early Cretaceous syn-transform phase (M3) characterized by significant clastic sediment accumulation on the Guinea Plateau and the highest
15 sedimentation rates on the plateau. Structural deformation, including strike-slip faulting and extensive subaerial erosion at the southwest of the plateau, corresponds with the opening of the EAG along the Guinea Fracture Zone. The Albian-Upper Cretaceous post-transform sequence (M4) is characterized by a major marine transgression and subsequent transgressive-regressive events. This was followed during the Cenozoic (M5) by
20 progressive subsidence and distal marine sedimentation, with lower sediment accumulation rates.

Dynamic topography likely played a significant role in the sedimentation pattern on the Guinea Plateau particularly on the second order 5-10 My duration transgressive-regressive cycles of the Upper Cretaceous and Paleogene, and to a lesser degree the deltaic complex in the Lower Cretaceous. Higher frequency third order (1 – 2 Myr) cycles are, however, likely controlled by global eustatic sea level changes.

20 Geochemical data suggest that enhanced organic carbon burial on the Guinea Plateau during the OAE2 perturbation is not related to a local nutrient trapping or other enrichment process known from deep ocean settings, but rather to excessive continental runoff linked to strong hydrological cycling and burial in an oxic environment, at least in the shallow area of the plateau. However, ongoing structural deformation near the Guinea Fracture Zone likely continued to impact ocean circulation through the emerging EAG during the
25 Cenomanian-Turonian.

Acknowledgements

We thank TGS Nopec, Schlumberger, and Office National des Pétroles (ONAP) in Guinea for access to 2D seismic and well data for this study. We also thank Schlumberger for use of an academic license of Petrel 2020 for seismic interpretation. BA acknowledges NDDC for PhD funding; UN, TW, TDJ and DD
30 acknowledge NERC grant number NE/W009927/1 for funding.

References

- Basile, C., & Mascle, J. (1990). Block faulting in oceanic crust: Example of intraplate deformation in the Equatorial Atlantic. *Marine Geology*, 95, 45 – 50.
- 5 Benkhelil, J., Mascle, J., & Huguen, C. (1998). Deformation patterns and tectonic regimes of the Côte d'Ivoire-Ghana transform margin as deduced from Leg 159 results. *Scientific Results*, 159.
- Berger, A., Fichet, T., Gallee, H., Marsiat, I., Tricot, C., & van Ypersele, J. (1990). Ice sheets and sea level change as a response to climatic change at the astronomical time scale. *R. Paepe et al. (eds.), Greenhouse Effect, Sea Level and Drought*, 85-107.
- 10 Berrocoso, Á. J., MacLeod, K. G., Martin, E. E., Bourbon, E., Londoño, C. I., & Basak, C. (2010a). Nutrient trap for Late Cretaceous organic-rich black shales in the tropical North Atlantic. *Geology*, 38(12), 1111–1114. <https://doi.org/10.1130/G31195.1>
- 15 Biari, Y., Klingelhoefer, F., Sahabi, M., Funck, T., Benabdellouahed, M., Schnabel, M., Reichert, C., Gutscher, M. A., Bronner, A., & Austin, J. A. (2017). Opening of the central Atlantic Ocean: Implications for geometric rifting and asymmetric initial seafloor spreading after continental breakup. *Tectonics*, 36(6), 1129–1150. <https://doi.org/10.1002/2017TC004596>
- Burgess, P. M., Winefield, P., Minzoni, M., & Elders, C. (2013). Methods for identification of isolated carbonate buildups from seismic reflection data. *AAPG Bulletin*, 97(7), 1071–1098. <https://doi.org/10.1306/12051212011>
- 20 Cartwright, J. A. (1994). Episodic basin-wide hydrofracturing of overpressured early Cenozoic mudrock sequences in the North Sea Basin. *Marine and Petroleum Geology*, 11(5)
- Casson, M., Jeremiah, J., Calvè, G., De Ville De Goyet, F., Reuber, K., Bidgood, M., Reháková, D., Bulot, L., & Redfern, J. (2021). Evaluating the segmented post-rift stratigraphic architecture of the Guyana continental margin. *Petroleum Geoscience*, 27. <https://doi.org/10.6084/m9>
- 25 Catuneanu Octavian (2019). Scale in sequence stratigraphy. *Marine and Petroleum Geology* 106 (2019) 128–159 <https://doi.org/10.1016/j.marpetgeo.2019.04.026>
- Chardon, D., Grimaud, J. L., Rouby, D., Beauvais, A., & Christophoul, F. (2016). Stabilization of large drainage basins over geological time scales: Cenozoic West Africa, hot spot swell growth, and the Niger River. *Geochemistry, Geophysics, Geosystems*, 17(3), 1164–1181. <https://doi.org/10.1002/2015GC006169>
- 30 Christopher M. Lowery, Jean M. Self-Trail, and Craig D. Barrie 2021 Enhanced terrestrial runoff during Oceanic Anoxic Event 2 on the North Carolina Coastal Plain, USA. *Climate of the Past*, 17, 1227–1242, 2021 <https://doi.org/10.5194/cp-17-1227-2021>
- Conrad, C. P., & Husson, L. (2009). Influence of dynamic topography on sea level and its rate of change. *Lithosphere*, 1(2), 110–120. <https://doi.org/10.1130/L32.1>
- 35 Davison, I. (2005). Central Atlantic margin basins of North West Africa: Geology and hydrocarbon potential (Morocco to Guinea). *Journal of African Earth Sciences*, 43(1–3), 254–274. <https://doi.org/10.1016/j.jafrearsci.2005.07.018>
- Dombrowski, J., Morgan, R., & Cameron, N. R. (2002). Could Guinea-Bissau (NW Africa) and not Brazil Host the First Amazon Delta? *AAPG Search and Discovery Article #90007*
- 40 Duarte, D., Nicholson, U., Aduomahor, B., Wagner, T., Dunkley Jones, T., Aptian-Albian opening of the Equatorial Atlantic Gateway: new evidence from Early Cretaceous sediment waves and contourite drifts west of the Guinea Plateau. *Earth and Planetary Science Letters* (in review)

- Dummann, W., Hofmann, P., Herrle, J. O., Frank, M., & Wagner, T. (2023). The early opening of the Equatorial Atlantic gateway and the evolution of Cretaceous peak warming. *Geology*, 51(5), 476–480. <https://doi.org/10.1130/G50842.1>
- 5 Dummann, W., Steinig, S., Hofmann, P., Flögel, S., Osborne, A. H., Frank, M., Herrle, J. O., Bretschneider, L., Sheward, R. M., & Wagner, T. (2020). The impact of Early Cretaceous gateway evolution on ocean circulation and organic carbon burial in the emerging South Atlantic and Southern Ocean basins. *Earth and Planetary Science Letters*, 530. <https://doi.org/10.1016/j.epsl.2019.115890>
- Emery and Myers (1996). *Sequence Stratigraphy*. Blackwell Science, Oxford, 297. <http://dx.doi.org/10.1002/9781444313710>
- 10 Erbacher, J., Mosher, D., & Malone, M. (2004). Drilling probes past carbon cycle perturbations on the Demerara rise. *Eos*, 85(6), 57–63. <https://doi.org/10.1029/2004EO060001>
- Friedrich, O., & Erbacher, J. (2006). Benthic foraminiferal assemblages from Demerara Rise (ODP Leg 207, western tropical Atlantic): possible evidence for a progressive opening of the Equatorial Atlantic Gateway. *Cretaceous Research*, 27(3), 377–397. <https://doi.org/10.1016/j.cretres.2005.07.006>
- 15 Frizon De Lamotte, D., Fourdan, B., Leleu, S., Leparmentier, F., & De Clarens, P. (2015). Style of rifting and the stages of Pangea breakup. *Tectonics*, 34(5), 1009–1029. <https://doi.org/10.1002/2014TC003760>
- Graindorge, D., Muséur, T., Klingelhoefer, F., Roest, W. R., Basile, C., Loncke, L., Sapin, F., Heuret, A., Perrot, J., Marcaillou, B., Lebrun, J. F., & Déverchère, J. (2023). Deep structure of the Demerara Plateau and its two-fold tectonic evolution: from a volcanic margin to a transform marginal plateau, insights from the Conjugate Guinea Plateau. *Geological Society, London, Special Publications*, 524(1), 339–366. <https://doi.org/10.1144/sp524-2021-96>
- 20 Guiraud, R., & Bosworth, W. (1997). Senonian basin inversion and rejuvenation of rifting in Africa and Arabia: Synthesis and implications to plate-scale tectonics. *Tectonophysics*, 282(1–4), 39–82. [https://doi.org/10.1016/S0040-1951\(97\)00212-6](https://doi.org/10.1016/S0040-1951(97)00212-6)
- 25 Haq, B. U. (2014). Cretaceous eustasy revisited. *Global and Planetary Change*, 113, 44–58. <https://doi.org/10.1016/j.gloplacha.2013.12.007>
- Heine, C., & Brune, S. (2014). Oblique rifting of the Equatorial Atlantic: Why there is no Saharan Atlantic Ocean. *Geology*, 42(3), 211–214. <https://doi.org/10.1130/G35082.1>
- 30 Heine, C., Zoethout, J., & Müller, R. D. (2013). Kinematics of the South Atlantic rift. *Solid Earth Discussions* <https://doi.org/10.5194/se-4-215-2013>
- Hendry, J., Burgess, P., Hunt, D., Janson, X., & Zampetti, V. (2021). Seismic characterization of carbonate platforms and reservoirs: An introduction and review. *Geological Society Special Publication*, 509 (1), 1–28. <https://doi.org/10.1144/SP509-2021-51>
- 35 Hofmann, P., Beckmann, B., Wagner, T. (2003). A millennial to centennial-scale record of African climate variability and organic carbon accumulation in the Coniacian-Santonian eastern tropical Atlantic (ODP Site 959, off Ivory Coast/Ghana). *Geology*, 31(2), 135-138. DOI: 10.1130/0091-7613(2003)031<0135:MTCSRO>2.0.CO;2.
- 40 Jarvis, I., Lignum, J. S., Grcke, D. R., Jenkyns, H. C., & Pearce, M. A. (2011). Black shale deposition, atmospheric CO₂ drawdown, and cooling during the Cenomanian-Turonian Oceanic Anoxic Event. *Paleoceanography*, 26(3). <https://doi.org/10.1029/2010PA002081>

- Jones, E. J. W., Bigg, G. R., Handoh, I. C., & Spathopoulos, F. (2007). Distribution of deep-sea black shales of Cretaceous age in the eastern Equatorial Atlantic from seismic profiling. *Palaeogeography, Palaeoclimatology, Palaeoecology*, 248(1–2), 233–246. <https://doi.org/10.1016/j.palaeo.2006.12.006>
- 5 Ko, J. (2018). Petroleum Geology of the Mauritania, Senegal, The Gambia, Guinea-Bissau, and Guinea-Conakry (MSGBC) Basin in the Northwest African Atlantic Margin. *Journal of the Korean Society of Mineral and Energy Resources Engineers*, 55(5), 478–490. <https://doi.org/10.32390/ksmer.2018.55.5.478>
- 10 Laugié, M., Donnadiou, Y., Ladant, J. B., Bopp, L., Ethé, C., & Raisson, F. (2021). Exploring the Impact of Cenomanian Paleogeography and Marine Gateways on Oceanic Oxygen. *Paleoceanography and Paleoclimatology*, 36(7). <https://doi.org/10.1029/2020PA004202>
- Leleu, S., & Hartley, A. J. (2010). Controls on the stratigraphic development of the Triassic Fundy Basin, Nova Scotia: Implications for the tectonostratigraphic evolution of Triassic Atlantic rift basins. *Journal of the Geological Society*, 167(3), 437–454. <https://doi.org/10.1144/0016-76492009-092>
- 15 Leleu, S., Hartley, A. J., van Oosterhout, C., Kennan, L., Ruckwied, K., & Gerdes, K. (2016). Structural, stratigraphic and sedimentological characterisation of a wide rift system: The Triassic rift system of the Central Atlantic Domain. *Earth-Science Reviews*, 158, 89–124. <https://doi.org/10.1016/j.earscirev.2016.03.008>
- 20 Liégeois, J.-P., Azzouni-Sekkal, A., Yahiaoui, R., & Bonin, B. (1990). The Hoggar swell and volcanism: Reactivation of the Precambrian Tuareg shield during Alpine convergence and West African Cenozoic volcanism. *Plates, plumes, and paradigms: Geological Society of America Special Paper* 388, 379–400
- Loncke, L., Mercier de Lépinay, M., Basile, C., Maillard, A., Roest, W. R., De Clarens, P., Patriat, M., Gaullier, V., Klingelhoefer, F., Graindorge, D., & Sapin, F. (2022). Compared structure and evolution of the conjugate Demerara and Guinea transform marginal plateaus. *Tectonophysics*, 822. <https://doi.org/10.1016/j.tecto.2021.229112>
- 25 Loncke, L., Roest, W. R., Klingelhoefer, F., Basile, C., Graindorge, D., Heuret, A., Marcaillou, B., Museur, T., Fanget, A. S., & Mercier de Lépinay, M. (2020). Transform Marginal Plateaus. *Earth Science Reviews*, 203. <https://doi.org/10.1016/j.earscirev.2019.102940>
- 30 Louis-Schmid, B., Rais, P., Schaeffer, P., Bernasconi, S. M., & Weissert, H. (2007). Plate tectonic trigger of changes in pCO₂ and climate in the Oxfordian (Late Jurassic): Carbon isotope and modeling evidence. *Earth and Planetary Science Letters*, 258(1–2), 44–60. <https://doi.org/10.1016/j.epsl.2007.03.014>
- Marinho, M., Mascle, J., & Wannesson, J. (1988). Structural framework of the southern Guinean Margin (Central Atlantic). *Journal of African Earth Sciences*, 7(2).
- 35 Marzoli, A., Renne, P. R., Piccirillo, E. M., Ernesto, M., Bellieni, G., & De Min, A. (1999). Extensive 200-million-year-old continental flood basalts of the Central Atlantic Magmatic Province. *Science*, 284(5414), 616–618. <https://doi.org/10.1126/science.284.5414.616>
- Mascle, J., Blarez, E., & Marinho, M. (1988). The shallow structures of the Guinea and Ivory Coast-Ghana transform margins: Their bearing on the Equatorial Atlantic Mesozoic evolution, *Tectonophysics*, 155(1–4), 193–209. [https://doi.org/10.1016/0040-1951\(88\)90266-1](https://doi.org/10.1016/0040-1951(88)90266-1)
- 40 Mercier de Lépinay, M., Loncke, L., Basile, C., Roest, W. R., Patriat, M., Maillard, A., & de Clarens, P. (2016). Transform continental margins – Part 2: A worldwide review. *Tectonophysics* 693, 96–115. <https://doi.org/10.1016/j.tecto.2016.05.038>

- Meyers, P. A., Bernasconi, S. M., & Forster, A. (2006). Origins and accumulation of organic matter in expanded Albian to Santonian black shale sequences on the Demerara Rise, South American margin. *Organic Geochemistry*, 37(12), 1816–1830. <https://doi.org/10.1016/j.orggeochem.2006.08.009>
- 5 Mitchum, R. M., & Vail, P. R., Sangaree, J. B. (1977). Seismic Stratigraphy and Global Changes of Sea Level: Part 6. Stratigraphic Interpretation of seismic reflection patterns in depositional sequences Section 2. Application of Seismic Reflection Configuration to Stratigraphic Interpretation. *AAPG Special Volume*, 165, 117-133
- 10 Moucha, R., Forte, A. M., Mitrovica, J. X., Rowley, D. B., Quéré, S., Simmons, N. A., & Grand, S. P. (2008). Dynamic topography and long-term sea-level variations: There is no such thing as a stable continental platform. *Earth and Planetary Science Letters*, 271(1–4), 101–108. <https://doi.org/10.1016/j.epsl.2008.03.056>
- Moulin, M., Aslanian, D., & Unternehr, P. (2010). A new starting point for the South and Equatorial Atlantic Ocean. *Earth-Science Reviews*, 98(1–2), 1–37. <https://doi.org/10.1016/j.earscirev.2009.08.001>
- 15 Moullade, M., Mascle, J., Benkhelil, J., Cousin, M., & Tricart, P. (1993). Occurrence of marine mid-Cretaceous sediments along the Guinean slope (Equamarge II cruise): their significance for the evolution of the central Atlantic African margin. *Marine Geology* (Vol. 110).
- Mourlot, Y., Calvès, G., Clift, P. D., Baby, G., Chaboureau, A. C., & Raison, F. (2018). Seismic stratigraphy of Cretaceous eastern Central Atlantic Ocean: Basin evolution and palaeoceanographic implications. *Earth and Planetary Science Letters*, 499, 107–121. <https://doi.org/10.1016/j.epsl.2018.07.023>
- 20 Nicholson, U., Bray, V. J., Gulick, S. P. S., & Aduomahor, B. (2022). The Nadir Crater offshore West Africa: A candidate Cretaceous-Paleogene impact structure. *Science Advances*, 8(33), eabn3096. [10.1126/sciadv.abn3096](https://doi.org/10.1126/sciadv.abn3096)
- Nicholson, U., Powell, W., Gulick, S., Kenkmann, T., Bray, V., Duarte, D., Collins, G., and Aduomahor, B. Into the Nadir: 3D anatomy of a K-Pg age marine impact crater. *Science Advances*, (In review).
- 25 Nicholson, U., Van Der Es, B., Clift, P.D., Flecker, R. and Macdonald, D.I., 2016. The sedimentary and tectonic evolution of the Amur River and North Sakhalin Basin: new evidence from seismic stratigraphy and Neogene–Recent sediment budgets. *Basin Research*, 28(2), 273-297.
- Olyphant, J. R., Johnson, R. A., & Hughes, A. N. (2017). Evolution of the Southern Guinea Plateau: Implications on Guinea-Demerara Plateau formation using insights from seismic, subsidence, and gravity data. *Tectonophysics*, 717, 358–371. <https://doi.org/10.1016/j.tecto.2017.08.036>
- 30 Pérez-Díaz, L., & Eagles, G. (2017). South Atlantic paleobathymetry since early Cretaceous. *Scientific Reports*, 7(1). <https://doi.org/10.1038/s41598-017-11959-7>
- Reuber, K. R., Pindell, J., & Horn, B. W. (2016). Demerara Rise, offshore Suriname: Magma-rich segment of the Central Atlantic Ocean, and conjugate to the Bahamas hot spot. *Interpretation*, 4(2), 141–155. <https://doi.org/10.1190/INT-2014-0246.1>
- 35 Rossi, S., Westall, F., & Mascle, J. (1992). The geomorphology of the Southwest Guinea Margin: tectonic, volcanic, mass movement and bottom current influences. *Marine Geology*, 105, 225-240
- Royston, S., Bingham, R. J., & Bamber, J. L. (2022). Attributing decadal climate variability in coastal sea-level trends. *Ocean Science*, 18(4), 1093–1107. <https://doi.org/10.5194/os-18-1093-2022>
- 40 Schlanger, S. O., Arthur, M. A., Jenkyns, H. C., & Scholle, P. A. (1987). The Cenomanian-Turonian Oceanic Anoxic Event, stratigraphy and distribution of organic carbon-rich beds and the marine ^{13}C excursion.

Marine Petroleum Source Rocks Brooks, J., Fleet, A. J. (Eds), *Geological Society Special Publication*, 26, 371-399

- Schlanger, S. O., & Jenkyns, H. C. (1976). Cretaceous Oceanic Anoxic Events: causes and consequences. *Geologie En Mijnbouw*, 55 (3-4), 179-184
- 5 Sclater, J. G., & Christie, P. A. F. (1980). Continental stretching: An explanation of the Post-Mid-Cretaceous subsidence of the central North Sea Basin. *Journal of Geophysical Research: Solid Earth*, 85(B7), 3711–3739. <https://doi.org/10.1029/jb085ib07p03711>
- 10 Sijp, W. P., von der Heydt, A. S., Dijkstra, H. A., Flögel, S., Douglas, P. M. J., & Bijl, P. K. (2014). The role of Ocean gateways on cooling climate on long time scales. *Global and Planetary Change* 119, 1–22. Elsevier. <https://doi.org/10.1016/j.gloplacha.2014.04.004>
- Tari, G., Molnar, J., & Ashton, P. (2003). Examples of salt tectonics from West Africa: a comparative approach. *Petroleum Geology of Africa: New Themes and Developing Technologies. Geological Society, London, Special Publications*, 207, 85-104.
- 15 Theodore R. Them, Benjamin C. Gill, David Selby, Darren R. Gröcke, Richard M. Friedman & Jeremy D. Owens (2017). Evidence for rapid weathering response to climatic warming during the Toarcian Oceanic Anoxic Event *Scientific Reports*, 7, 5003. DOI:10.1038/s41598-017-05307-y
- Topper, R. P. M., Trabucho Alexandre, J., Tuenter, E., & Meijer, P. T. (2011). A regional ocean circulation model for the mid-Cretaceous North Atlantic Basin: Implications for black shale formation. *Climate of the Past*, 7(1), 277–297. <https://doi.org/10.5194/cp-7-277-2011>
- 20 Trabucho Alexandre, J., Tuenter, E., Henstra, G. A., Van Der Zwan, K. J., Van De Wal, R. S. W., Dijkstra, H. A., & De Boer, P. L. (2010). The mid-Cretaceous North Atlantic nutrient trap: Black shales and OAEs. *Paleoceanography*, 25(4). <https://doi.org/10.1029/2010PA001925>
- 25 Voigt, S., Jung, C., Friedrich, O., Frank, M., Teschner, C., & Hoffmann, J. (2013). Tectonically restricted deep-ocean circulation at the end of the Cretaceous greenhouse. *Earth and Planetary Science Letters*, 369–370, 169–177. <https://doi.org/10.1016/j.epsl.2013.03.019>
- Wagner, T., & Pletsch, T. (1999). Tectono-sedimentary controls on Cretaceous black shale deposition along the opening Equatorial Atlantic Gateway (ODP Leg 159). *Geological Society, London, Special Publications*, 153, 241-265
- 30 Wagner, T. (2002). Late Cretaceous to early Quaternary organic sedimentation in the eastern Equatorial Atlantic. In *Palaeogeography, Palaeoclimatology, Palaeoecology*, 179.
- Wagner, T., Sinninghe Damsté, J., Beckmann, B. and Hofmann, P. (2004). Euxinia and primary production in Upper Cretaceous eastern equatorial Atlantic surface waters fostered orbital-driven formation of marine black shales. *Paleoceanography*, 19, 4099. doi:10.1029/2003PA000898
- 35 Wagner T. (2006). Insolation-control on the Late Cretaceous hydrological cycle and tropical African climate - global climate modelling linked to marine climate records. *Palaeogeography-Palaeoclimatology-Palaeoecology*, 235, 288-304.
- Withjack, M. O., & Schlische, R. W. (2005). A Review of Tectonic Events on the Passive Margin of Eastern North America. *Society of Economic Paleontologists and Mineralogists*. <https://doi.org/10.5724/gcs.05.25.0203>
- 40 Wright, N. M., Seton, M., Williams, S. E., Whittaker, J. M., & Müller, R. D. (2020). Sea-level fluctuations driven by changes in global ocean basin volume following supercontinent break-up. *Earth-Science Reviews*, 208. <https://doi.org/10.1016/j.earscirev.2020.103293>

Xia, Y., Yang, J., Chen, Y., Lu, S., Wang, M., Deng, S., Yao, Z., & Lu, M. (2022). A review of the global polygonal faults: Are they playing a big role in fluid migration? *Frontiers in Earth Science*, 9. <https://doi.org/10.3389/feart.2021.786915>

5 Young, A., Flament, N., Williams S. E., Meredith, A., Cao, X and Müller, R. D. (2022). Long-term Phanerozoic Sea level change from solid Earth processes. *Earth and Planetary Science Letters* 584 (2022)117451 <https://doi.org/10.1016/j.epsl.2022.117451>

Zimmerman, H. B., Boersma, A., & Mccoy, F. W. (1987). Carbonaceous sediments and palaeoenvironment of the Cretaceous South Atlantic Ocean. Marine Petroleum Source Rocks. *Geological Society Special Publication*, 26, 271-286

10

15

20

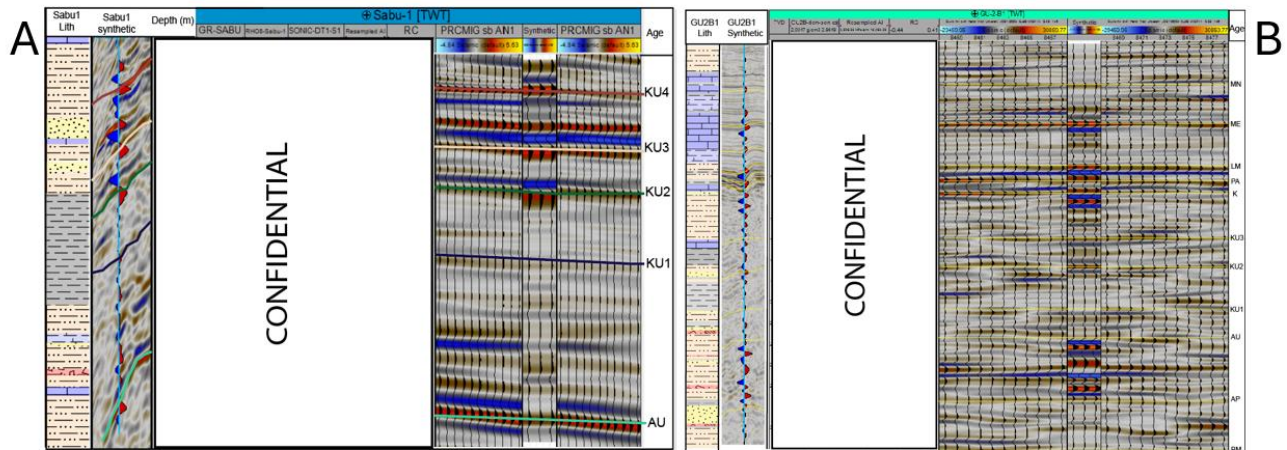
25

30

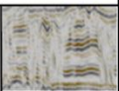
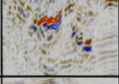
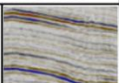
Supplementary materials

A1: Seismic acquisition parameters for the three seismic surveys on the Guinea margin

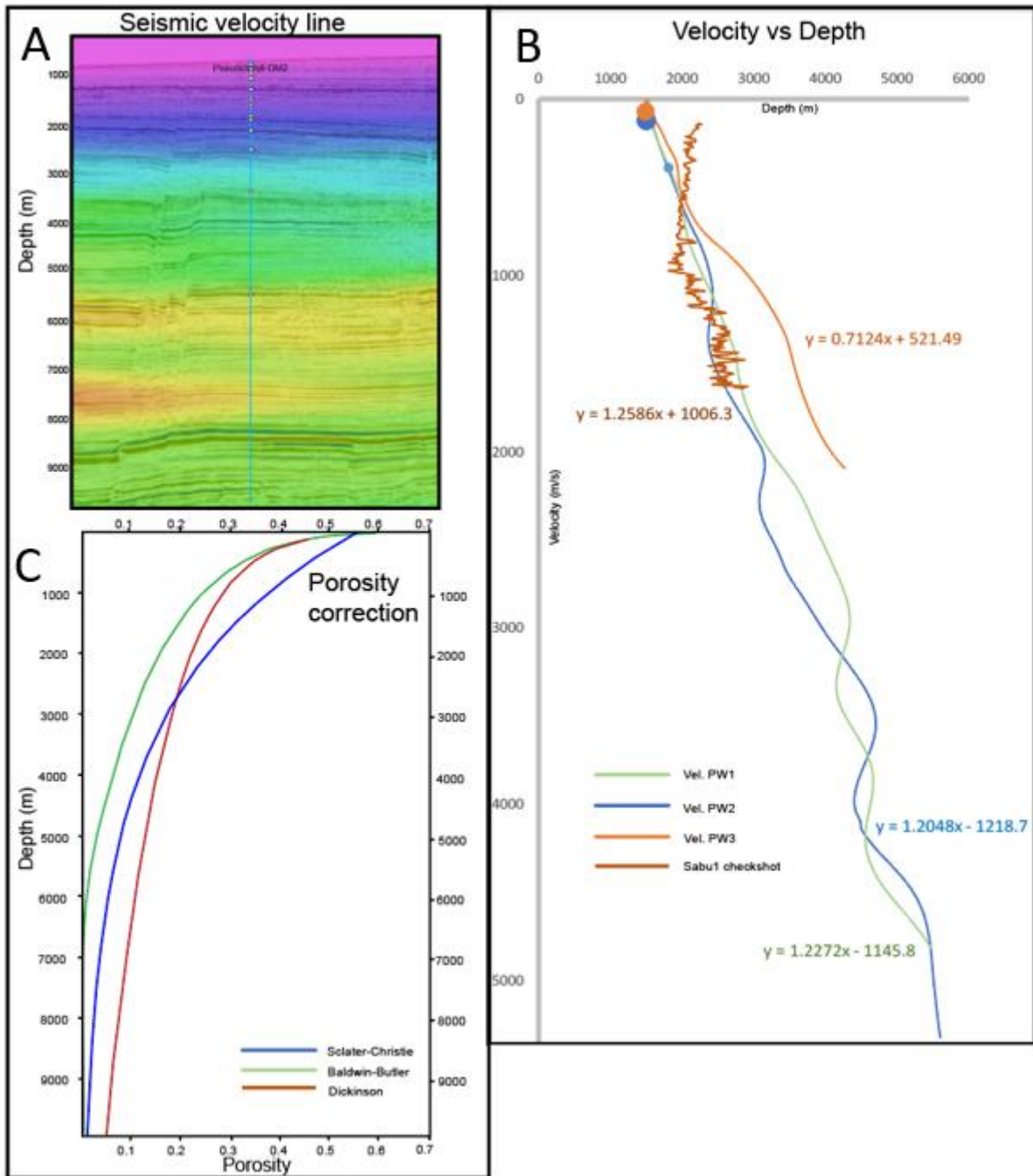
Acquisition parameter	NWAAM17 (Survey 1)	NWAAM17 (Survey 2)	GWG99
Streamer length	8km	12 km	6 km
Streamer depth	8m	18m	8 m
No. of channels	640	960	480
Airgun volume	4330 in 3 arrays	4310 in 3 arrays	2000 in 3 arrays
Gun depth	6 m	8 m	6 m
Shot point interval	25 m	25 m	25 m
Group interval	12.5 m	12.5 m	12.5 m
No. of fold	160	240	120
Record length	9 seconds	14 seconds	10 seconds
Sampling interval	2 ms	2 ms	4 ms
Sample rate	4 ms	4 ms	2 ms



A3: Seismic to well tie for A) Sabu-1 and B) GU2B-1 wells

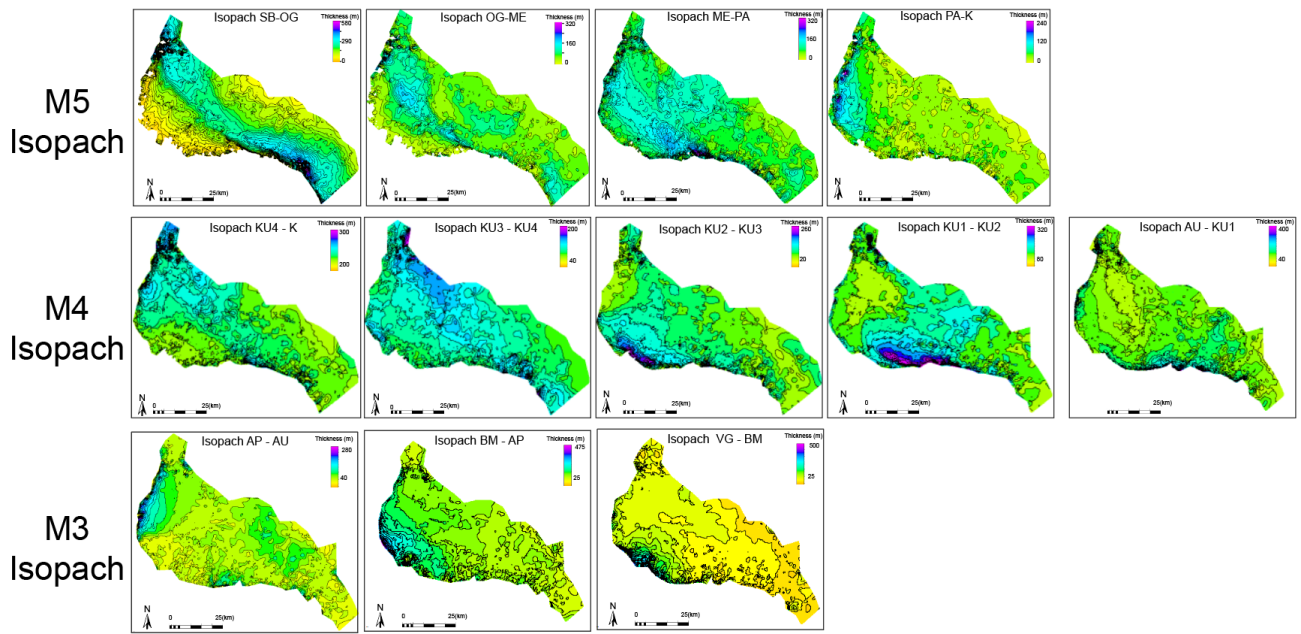
Seismic Facies	configuration and continuity	Amplitude and frequency	Interpretation/environment
I	 Parallel to sub-parallel, discontinuous, blocks bounded by internal chaotic reflection	Low to medium amplitude blocks surrounding low amplitude, low frequency, chaotic unit	Mass Transport Complex (MTC)
II	 Parallel to subparallel truncated discontinuous	Low to medium amplitude, medium to high frequency	Polygonal faults Siliceous mudrocks
III	 Abrupt lateral termination	Very high amplitude, low frequency	Magmatic sills
IV	 Chaotic, transparent, incoherent, overlapped by parallel to subparallel reflectors	Very high amplitude, low frequency	Volcanoes
V	 Oblique, wavy, discontinuous, parallel to subparallel	Low to medium amplitude, low to medium frequency	Prograding clinoform delta
VI	 Chaotic, transparent, incoherent, flanked by parallel to subparallel reflectors	Low frequency, low amplitude Vertical zone of discontinuity (VZD)	Magma conduit
VII	 Chaotic, transparent, incoherent	Low frequency, low amplitude	Salt diapirs
VIII	 Parallel, wavy, downdip	Low frequency, low amplitude	Contourite drift
Seismic Facies	configuration and continuity	Amplitude and frequency	Interpretation/environment
IX	 Parallel to sub-parallel, continuous	Medium to high amplitude, low to high frequency	Carbonate platform
X	 Undulating, stepping to wavy reflectors	Low to medium amplitude, low to medium frequency	Sediment waves
XI	 Non-reflective, transparent, discontinuous	High amplitude at the top, low amplitude internally, low frequency	Crystalline basement
XII	 Oblique, diverging, continuous to discontinuous, seaward dipping	Medium to high amplitude, medium to high frequency	SDRs
XIII	 Parallel, horizontal, laterally continuous	Low to medium amplitude, medium to high frequency	slope shale
XIV	 Parallel to subparallel, continuous reflectors	Medium to high frequency, low amplitude	Pelagic or hemipelagic shale
XV	 Chaotic, incoherent, discontinuous, wedge-shaped	Low to medium frequency medium to high amplitude	Blocky talus from carbonate platform
XVI	 Dense updip, high angle discontinuous truncating reflectors	Low to medium amplitude, medium to high frequency	Strike slip fault

A4: Seismic facies model generated for this study.



A5: Workflow for time-depth conversion and porosity correction for calculating sediment accumulation rates. (a) seismic velocity profile of one of the pseudo wells. Processing velocities were extracted from the seismic velocities along a vertical trace. (b) Extracted processing velocity plotted against checkshot data from offshore well. (c) porosity-depth profiles used to reconstruct solid sediment volumes. Image from 2D Move.

5



A6: Isopach maps for the major intervals used for the sediment budget calculation. Contour interval is 50 m.